School of Industrial Engineering and Management

Hybrid Joining of Aluminum to Thermoplastics with Friction Stir Welding

Master of Science Thesis
by
Wallop Ratanathavorn

Department of Materials Science and Engineering
KTH-Royal Institute of Technology
Stockholm, Sweden

ABSTRACT

Hybrid structures including aluminum-thermoplastic and aluminum-reinforced thermoplastic composite are increasingly important in the near future innovations due to its lightweight and high strength-to-weight ratio. A critical point for metal-polymer application is that sound joining of these materials is difficult to achieve owing to a large difference in surface energy and dissimilar structure between metal and polymer. In practice, two major joining methods for hybrid structures are mechanical joining and adhesive bonding. However, there are some drawbacks of these conventional methods such as stress concentration, long curing time and low reliability joints. A new novel metal-polymer hybrid joining is required to overcome these issues as well as manufacturing and cost perspectives.

To this end, this work aims to develop a general methodology to apply friction stir welding techniques to join a wide range of thermoplastics with and without fibers to aluminum alloy sheets. The present work proposed an experimental study to attain insight knowledge on the influences of welding parameters on the quality of hybrid joints in term of the maximum tensile shear strength. This includes the role of tool geometries, welding methodology as well as material weldability in the investigation. The results showed that friction stir welding is a promising technique for joining of thermoplastic to aluminum. Microstructural observation showed that a good mixing between aluminum and thermoplastic as well as defect-free weldments were obtained. Tool geometries and welding speed are two factors that significantly contribute to the quality of friction stir welded hybrid joints. The results also demonstrated that weld fracture modes are associated with material mixing as well as interfacial bonding between aluminum and thermoplastic.

An evaluation of the joint strength was benchmarked with the relevant literatures on hybrid joining. The results of proposed technique showed that the maximum tensile shear strength of friction stir welded joints were the same order of magnitude as the joints welded by laser welding.

Keywords: friction stir welding, hybrid welding

ACKNOWLEDGEMENTS

LIST OF ACRONYMS

ABS	Poly(Acrylonitrile, Butadiene, Styrene)
AS	Advancing side
CCW	Counterclockwise direction
CFRP	Carbon-fiber-reinforced polymer
CW	Clockwise direction
DSC	Differential scanning calorimetry
DTB	Distance to backing
FSLW	Friction stir lap welding
FSpJ	Friction spot joining
FSSW	Friction stir spot welding
FSW	Friction stir welding
GFRP	Glass-fiber-reinforced polymer
HAZ	Heat affected zone
HDPE	High-density polyethylene
PA	Polyamide
PET	Polyethylene terephthalate
PP	Polypropylene
PPS	Polyphenylene sulfide
RS	Retreating side
RSW	Resistance spot welding
SEM	Scanning electron microscope
TMAZ	Thermomechanically affected zone
TWI	The welding institute (UK)
UHMW	Ultra High Molecular Weight

TABLE OF CONTENTS

1. INTRODUCTION

1.1 Background

Lightweight structures are increasingly important in variety of applications. They are used as body parts in modern automobile structures or as reinforced plastics wing or fuselage sections in modern aviation structures. In addition, composite materials such as carbon-fiber-reinforced polymer (CFRP) or glass-fiber-reinforced polymer (GFRP) are also integrated to lightweight metals such as aluminum or magnesium for a very strong and lightweight hybrid structure. However, joining between dissimilar materials especially metal-polymer joining is still a main issue in the development of new advanced hybrid structures.

Fig. 1 Hybrid structures of thermoplastic composites and metals in automotives applications [1].

Currently, one of the major joining methods for metal-polymer hybrid structures is mechanical joining. This method can be used to join variety of dissimilar materials together including metal to metal, polymer to polymer and metal to polymer. The strong advantage of mechanical joining is that the joints can be disassembled in case of repair or modification. However, stress concentration near holes of riveted joints can lead to crack formation or crack propagation inside the materials. In addition, the weight of mechanical fasteners such as bolts or rivets will increase the overall weight of the structures.

Adhesive bonding is another method widely used for metal-polymer hybrid joining at present. This method gives many advantages in material joining including uniform stress distribution, small distortion effect, ability to join almost any combination of materials, ability to join complex joint geometry and ability to control physical properties of joints [2]. The strength of adhesive bonding joints strongly depends on surface free energy and

wettability of materials [2]. The higher the surface free energy, the better the adhesive bonding they can reach. Adhesive bonding joints of metal-polymer hybrid structures are more likely to have the problems due to large surface free energy difference and very low surface free energy of polymers. The following table shows the surface free energy of common used materials.

Table 1: Surface free energy value for some common materials [2]

Solid surface	Surface free energy γ_s (mJ/m^2)
PTFE	19.1
Polypropylene	30.2
Polyethylene	32.4
Polystyrene	40.6
PMMA	40.2
Nylon 6,6	41.4
PVC	41.5
PET	45.1
Epoxy (averaged)	~46
Carbon fibre reinforced plastic (abraded)	58.0
Silica	287
Alumina	~620
Fe$_2$O$_3$	1357
Copper	1360

Welding is a developing method to join metal-polymer hybrid structures at the present. This joining technique has many strong advantages over conventional joining methods such as mechanical joining and adhesive bonding. It requires less surface preparation, shorter processing time and also less chemical wastes when comparing with two conventional methods. In the work of Amancio-Filho and Santos [3], they reviewed present welding literatures on polymers and metal-polymers joining that have already been published. Friction Riveting [4] is one of newly developed techniques for joining dissimilar materials proposed by Amancio-Filho et al. The rotating metal screw rivet is used to penetrate the metal-polymer structures. When it reaches the desired penetration depth, the rotation speed will abruptly increase to generate more frictional heat. The rivet tip will consequently be plastically deformed by heat softening, the metal and polymer are finally held together. This method can reduce the stress concentration from drilled holes, however; it can be used to join in spot joints only.

Friction Stir Welding (FSW) is a successful method that is typically used to join aluminum and some lightweight alloys such as magnesium and titanium. It is a solid-state welding method that uses rotating tool to generate heat and forge the plasticized materials into joint line for consolidation. The stirred materials are softened by frictional heat mainly from work-piece and shoulder surfaces. Without melting, FSW can visibly solve the conventional problems in fusion welding such as porosity, distortion or

solidification cracking with very good mechanical properties especially fatigue strength due to unchanged material microstructure. In addition, FSW can be effectively used to join a variety of thermoplastic materials by the method proposed by Nelson et al. [5]. The details of friction stir welding literatures including polymer and metal-polymer welding will be illustrated in chapter 2.

1.2 Objectives

The aim of this thesis is to develop the fundamental knowledge on the possibilities to apply friction stir welding techniques to join a variety of thermoplastics to aluminum alloy sheets by using the conventional FSW tools.

In order to understand the metal-thermoplastics welding, the effects of welding parameters are investigated. The maximum tensile shear strength of friction stir welded joints will be benchmarked with the relevant literatures on hybrid joining.

1.3 Scope and limitations

This thesis focuses on the applicability of friction stir welding process for joining metal-thermoplastic sheets. In order to understand the effect of welding variables, the mechanical joint strength and joint structure are investigated. The joint configuration used in this thesis is limited to lap joint configuration. The FSW tools used in the experiments are based on the existing FSW tools at ESAB laboratory. There is no tool development included in this thesis.

2. LITERATURE REVIEW

In this chapter, the basic principles of friction stir welding processes and the existing literatures on polymer and metal-polymer welding are illustrated. The focused welding methods across this chapter are based on lap welding including friction stir lap welding and friction stir spot welding. In the first section, the fundamental knowledge of friction stir welding is reviewed. This section is followed by the extensive works on friction stir welding of lap joints for metal to metal joining. The research works on friction stir spot welding is also investigated in the third section. For the rest of the chapter, the extensive works on polymers and polymer-metal hybrid welding are reported. Currently, polymeric materials such as polypropylene and ABS have been successively joined by friction stir welding technique [5]. However, there are few cases so far for an achievement of polymer-metal hybrid welding.

2.1 Friction stir welding basic principles

Friction stir welding is a solid-state welding method that was invented by Thomas W.M. at The Welding Institute (TWI) in United Kingdom. At the initial state, it was used for welding of aluminum and aluminum alloys applications. To date, FSW has been used as a common welding technique for other lightweight metals such as magnesium and titanium alloys. It was proven that it results in low distortion of work-pieces, high joint strength and low porosity especially in joining of active metals such as aluminum or magnesium. The basic principles of FSW are rather simple compared to other conventional fusion welding techniques. FSW uses a rotating non-consumable tool with shoulder and pin to insert into the work-piece, transverse along the joint line and retract from the plates as shown in Fig. 2.
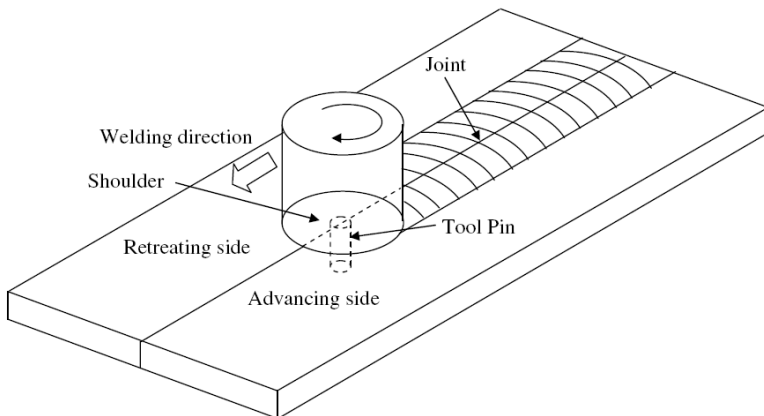

Fig. 2 The basic principles of friction stir welding of a butt joint [6].

Friction stir welding is a thermomechanical process that involves the complex interactions between different phenomena and varies throughout the weld regions [6, 7]. Generally, friction stir welded material can be divided into four regions as shown in Fig. 3. In the heat affected zone (HAZ), there is no plastic deformation; however, metallurgical microstructure and mechanical properties of parent material are modified by the heat generated from the weld-center. In the thermomechanically affected zone (TMAZ) and the stirred zone, the combination of plastic deformation, dynamic recrystallization and recovery occur simultaneously during the process [6]. Whilst the deformed grains are still retained in TMAZ, fully recrystallization significantly occurs in the stirred zone only.
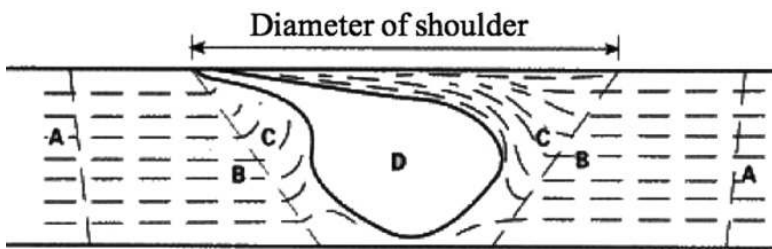

Fig. 3 The schematic shows different regions of the cross section of friction stir welded material. A) Parent material B) Heat affected zone (HAZ) C) Thermomechanically affected zone (TMAZ) D) Stirred zone [8].

One of the main factors that controls mass and heat transport inside the friction stir welded material is a rotating tool. It involves three functions in friction stir welding process, heating weld material, transporting plasticized material and constraining soften material [7]. Heat is generated during the friction stir welding process by severe plastic deformation of the work-piece and frictional heat between the rotating tool-weld material surfaces [6, 7]. The process can be considered as a keyhole welding process where the plasticized material being welded is transported from the leading edge to the backside of the tool where it is consolidated by the forging pressure from the shoulder to the work-piece. These phenomenas can be regarded as extrusion and forging processes of metal by the rotating FSW tool.

There are many advantages of friction stir welding over the conventional welding in terms of properties, eco-friendly and economy [9]. FSW can be used for most joint configurations in contrast to conventional friction welding. It can also weld variety of alloys with low distortion, absence of solidification cracking, uniform alloying element and excellent mechanical properties especially fatigue strength. Friction stir welding operation requires no shielding gas, no consumable materials such as wire, rugs or any filler materials. It also uses low energy without any toxic fumes and slag wastes.

In this project, the lap joint configuration was used for friction stir welding of metal-thermoplastic hybrid structures. To focus on this specific application, friction stir lap welding will be illustrated in detail in the next section.

2.2 Friction stir lap welding (FSLW)

The conventional friction stir welding process was successfully used to join aluminum butt welding in variety of applications such as ship building and aerospace fabrication. However, lap joining which is the replacement of mechanical fasteners such as bolts and rivets is also widely used in industrial applications. In contrast to butt welding, sound friction stir lap welding is more difficult to achieve by typical pin tools because: 1) thinning of the upper sheet due to severe uplift material at advancing side. 2) the oxide layer is difficult to break up due to the parallelism between oxide layer and horizontal material flow velocity [7]. TWI has overcome these disadvantages of the conventional butt joint tools by developing the new tool geometries called Flared-Triflute and Skew-stir tools as shown in Fig.4.

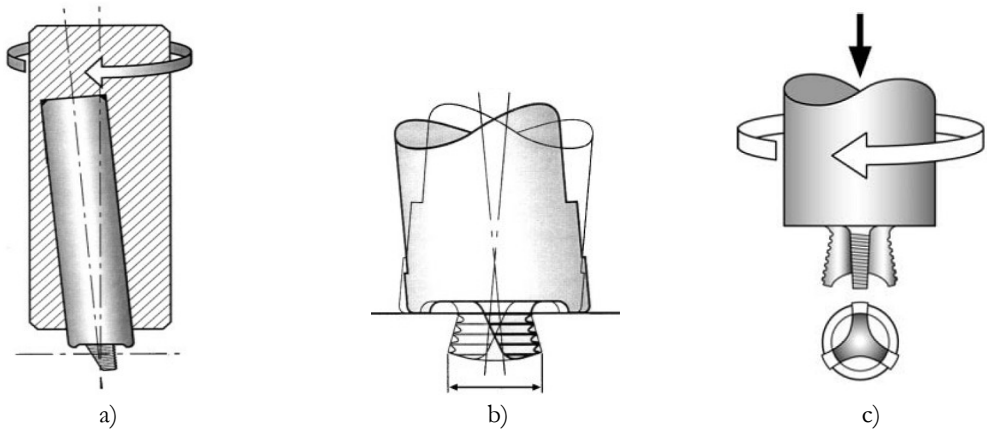<div align="center">a)　　　　　　　　　　　b)　　　　　　　　　　　c)</div>

Fig. 4 Friction stir lap welding tools developed by TWI. a) Skew-stir tool b) Swept region by Skew-stir tool c) Flared-Triflute tools [10, 11].

For Skew-stir tool, the motion of A-skew probe as shown in Fig.4b can enhance the plastic deformation of the work-piece material resulting in an improvement of oxide layer disruption and lower weld defects formation [11]. The variants of Skew-stir tool can be illustrated by the position of the focal point which is an intersection between machine spindle axis and skew probe axis. If the focal point is on the work-piece top surface, the probe will rotate in rotary motion only. However, when the focal point is above or below the work-piece top surface, the probe will rotate in both rotary and orbital motion.

The micrographs investigation showed that there are interfaces between the upper and lower plates on both advancing and retreating sides in all specimens. The reason to this is associated with the residual oxide layer on the surface and oxide film formation during friction stir welding [11]. The presence of oxide layers causes partially bonding instead of fully bonding during the original faying surface consolidation. As a result, the interfaces are formed leading to weaker mechanical properties and undesirable fracture path of the weldments.

The tensile test results revealed that Skew-stir tool gives twice maximum tensile loads comparing with the results achieved by conventional threaded pin tool. The higher maximum tensile loads were due to desirable interface location and greater bonding area on the fracture surface [11]. The cross sections of joints welded by Skew-stir tool and conventional threaded pin tool are shown in Fig.5. The fracture paths are indicated by the white lines on the figures.
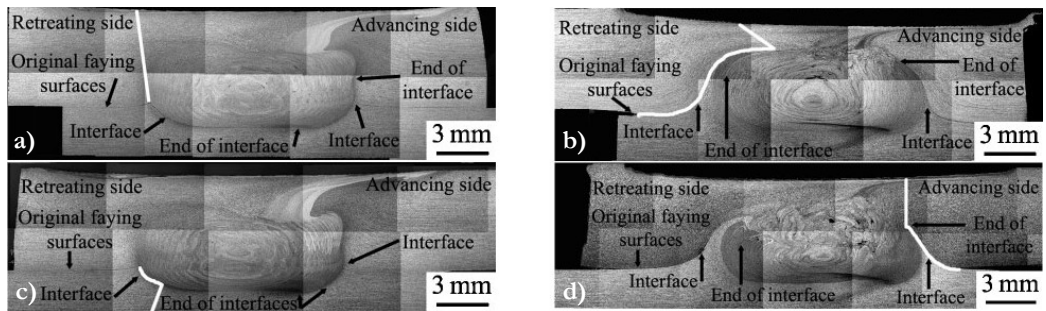

Fig. 5 Macrographs of joint cross sections welded by different tools. a) Right-hand Skew-stir tool joint b) Right-hand conventional threaded pin tool joint c) Left-hand Skew-stir tool joint d) Left-hand conventional threaded pin tool joint [11].

In friction stir lap welding of thin sheets, the size of shoulder plays an important role in joint properties rather than pin or probe. Zhang et al. [12] reported the interfacial bonding is achieved by oxide layer disruption and vertical intermixing of material by rotating shoulder.

Two large featureless shoulder tools (15, 20 mm) without pin were used to investigate the role of shoulder on bonding area and its mechanism. The results showed that the larger shoulder diameter can improve both joint surface appearance and joint properties while the absence of pin has no significant effects on heat generation and weld cross section microstructure. The role of wide shoulder on interfacial bonding is called boundary effect by the authors. This boundary effect causes vertical intermixing and interfacial bonding with dense structure especially near the weld boundary as shown in Fig.6b.

The bonding area of wide shoulder tool is similar or superior comparing with probe tool. However, the bonding of material can be well achieved only near the weld boundary while it was poor at the central region. The reason is from a lack of torsion action which is the result of tangential material flow driven by shoulder and the forging effect. The level of tangential flow depends on two factors: linear velocity and tool axial load. When the tool axial load is increased up to a certain value, the material in sub-surface layer will be dragged by rotating shoulder in the tangential direction. This shoulder-driven flow causes velocity gradient at the bonding interface resulting in an oxide disruption. However, at the central region, the linear velocity is too low; therefore, the level of tangential flow is also weak to induce metal flow within upper plate. Consequently, the interfacial bonding at the central region across the thickness cannot be well achieved.
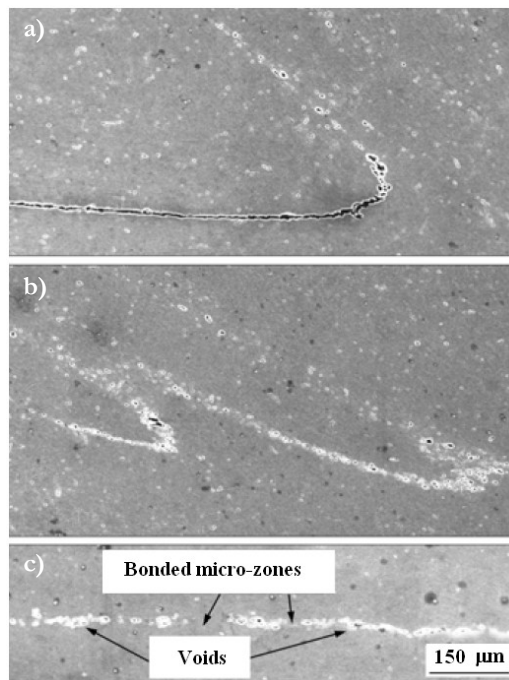
Fig. 6 Micrographs of specimen cross sections of FSLW joints welded by 15-mm-shoulder tool: a) weld boundary b) inside weld boundary c) central region [12].

2.3 Friction stir spot welding (FSSW)

In modern vehicle body structures, sheet metals are widely used as closure panels in pillars, hoods or door panels. The closure components made of steel sheets are normally joined by conventional resistance spot welding (RSW). However, an increasing in weight reduction requirement from fuel economy improvement leads to the replacement of material from steel to lightweight alloys such as aluminum or magnesium. Conventional RSW has been proved that it is not suitable for joining lightweight alloys due to its high heat input which induces high distortion and defect formation inside the joints. Recently, friction stir spot welding (FSSW) has shown that it is an alternative method for spot welding of lightweight alloys due to its low heat input, low operating costs, short cycle time and good weld strength [13].

The friction stir spot welding can be classified into three categories [13]: Pure FSSW, Refill FSSW [15] and Swing FSSW [16]. Pure FSSW uses conventional friction stir welding tools with or without probe to penetrate into the work-piece, hold for a certain duration and finally withdraw from the work-piece as shown in Fig. 7. This method was firstly used in the real production line for Mazda RX-8 rear door panel in 2003 [14]. The main advantages of pure FSSW over conventional RSW are lower investment costs, better mechanical properties and lower energy consumption. The key parameters that determine the weld strength of pure FSSW joints are rotation speed, tool plunge depth and holding time [17, 18]. The optimum tool plunge depth is suggested to be the value that the pin plunges approximately 25 percent of the bottom sheet thickness [19].
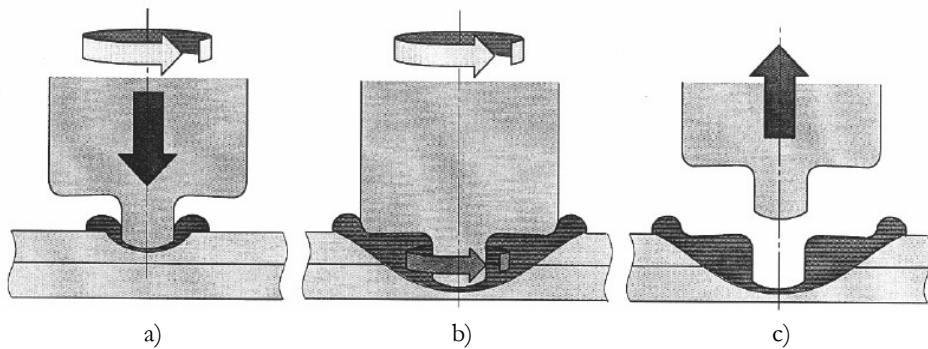

Fig. 7 Pure FSSW principles with probe tool. a) Plunging. b) Holding. c) Withdrawing. [20].

When the rotating tool plunges into the work-piece, the metal is drawn upward along the pin periphery by backward extrusion phenomena. However, by the pressure from shoulder surface, the metal is pushed downward and hook is formed at the interface between upper and bottom sheet. The hook formation as well as plastic flow are dependent on tool geometry used in FSSW [18]. S. Hirasawa et al. analyzed the effect of

various tool geometries on material flow during FSSW by use of simulation together with experimental results. The results showed that triangular pin gives enhanced upward plastic flow compared with cylindrical pin tool due to its strong plastic deformation by asymmetric pin shape. They also reported that triangular pin can enhance the mixing of materials due to the different horizontal flow between the corner and the surface of the pin. The strength of joints welded by triangular and cylindrical pin tools are investigated by Badarinarayan et al. [17]. The results showed that the weld strength of triangular pin joint is twice higher than cylindrical pin joint in cross-tension test. The reasons are from the difference in failure mode due to different hook geometry and also the grain size after spot welding of triangular pin joint is finer than cylindrical pin joint which gives rise to higher material strength.

One limitation of pure FSSW comparing with conventional RSW is it leaves pin hole behind after spot welding. Many studies have tried to develop alternative methods for FSSW without pin hole, however; if the pure FSSW tool has no pin, the material can flow vertically just only 0.5 mm depth from the shoulder surface [21]. This insufficient penetration into the bottom sheet leads to low energy failure by shear mode due to weak bonding along the weld line.

Tozaki et al. [22] have proposed a newly developed tool which uses scroll groove to displace the material in vertical direction instead of profiled pin. The experimental results showed that scroll groove tool without pin gives equally or superior results compared with conventional convex shoulder tool with cylindrical pin. They also investigated the importance of scroll groove on plasticized material flow by comparing with convex plain shoulder tool without pin. The results showed that plain tool gives very weak bonding between upper and lower plate while scroll groove tool gives very good bonding at interface as visibly seen by micrographs. The downward material flow can also be seen in scroll groove tool joints only. The schematics of proposed tool by Tozaki et al. are shown in Fig. 8.
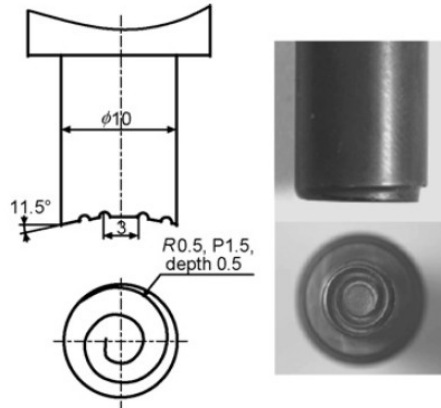
Fig. 8 Dimensions and tool configuration developed by Tozaki et al. [22].

A study of Bakavos et al. [23] gives very deep insight into material interaction in FSSW with pinless tools. Their study used five novel pinless tools as shown in Fig. 9 to investigate the material flow and mechanisms of weld formation of 0.93-mm-thick AA6111 spot joints. The results showed that the long flute wiper tool gives highest failure energy among all the pinless tools while the flat tool gives the lowest one.
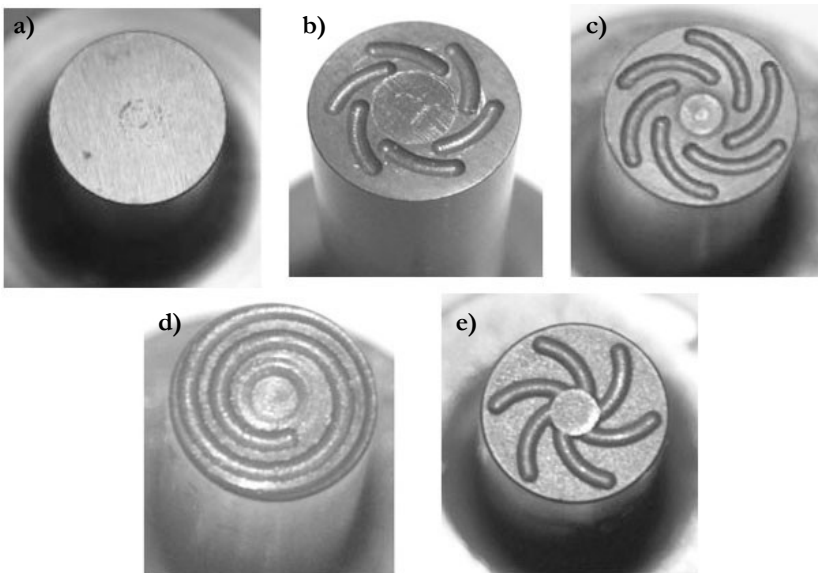

Fig. 9 The pinless tools configuration with 10-mm-shoulder diameter used in friction stir spot welding of thin AA6111-T4 sheets: a) flat tool b) short flute wiper tool c) long flute wiper tool d) scroll tool and e) proud wiper tool [23].

The material flow investigation results showed that the flute wiper tool and scroll tool give very good material penetration into the bottom sheets while the flat tool gives only shallow penetration just below the weld line. The results also showed that the penetration depth can be increased by the longer tool holding time. However, very long tool holding time (greater than 1 second) will give rise to hook formation by higher radial flow which causes lower pull out failure energy. They suggested that the depth of penetration and the level of hooking should be balanced by the tool holding time in order to achieve the highest weld strength.

Although, the surface features such as flute wiper and scroll surfaces can increase the penetration depth of material into the bottom sheets, they also lead to weld defect formation inside the welds. The failure load testing results of all tool features as shown in Fig.10 gives unexpected results that the scroll tool weld strength is among the lowest group even it has a very good material penetration. The reason for low weld strength of this tool is from a large circumferential cracking near the weld edge. The cracking occurs during the initial plunging of the tool while the top sheet is not sufficiently hot. The high contact friction of the top sheet and scroll groove while it is cold causes very high shear stress below the tool surface. When the disk tries to rotate, the shear cracking will be formed near the tool periphery. They suggested that this circumferential cracking can be eliminated by slower plunge rate in order to let the sheet temperature to be sufficiently hot.
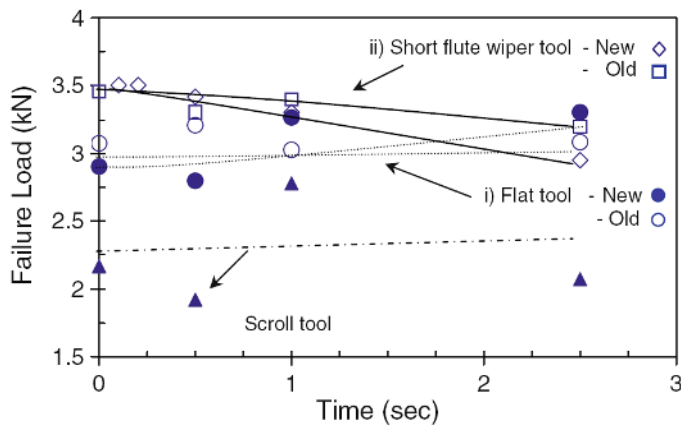

Fig. 10 The failure load graph of pinless tools with different tool holding time. [23]

The second technique in FSSW which can fulfill the need in spot welding without pin hole is refill FSSW invented by GKSS [15]. This technique uses a retractable pin which can move independently from the shoulder when plunging into the work-piece. After the retractable pin is plunged, the material is displaced by backward extrusion upward

towards the shoulder similar to conventional FSW. The pin is then retracted and both pin and shoulder push the displaced material back for consolidation. The experimental results also showed that refill FSSW can improve tensile strength of joints by approximately 30% compared with FSSW with probe hole under the same parameters [24]. The increased tensile strength was due to greater cross section area when the probe hole was filled. The refill FSSW processes illustration is shown in Fig. 11.

In pure FSSW, a rotating tool plunges into the work-piece, holds for a certain of time and retracts from the work-piece. Instead of only holding for a certain of time, stitch and swing FSSW translate the tool in a short distance before retracting [13]. This translating results in an increased weld area between upper and lower sheets which can improve the strength of the joint [16].
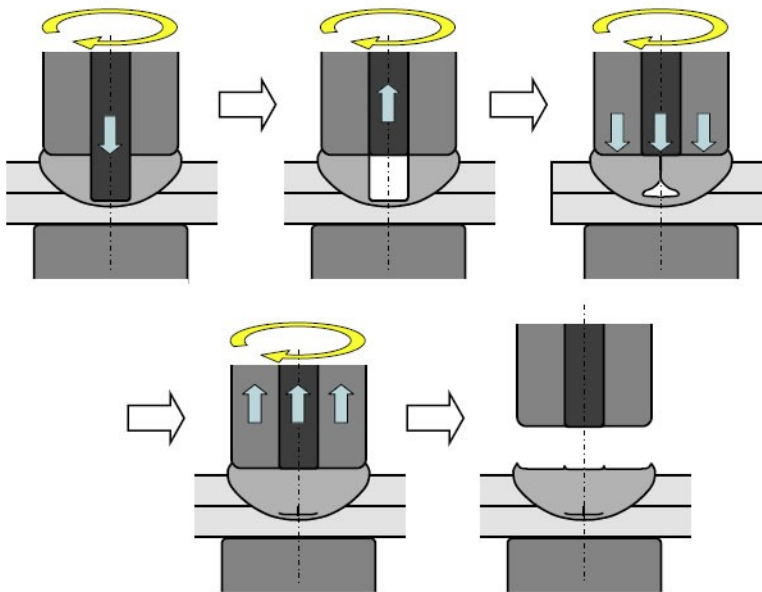
Fig. 11 Refill FSSW principles [24].

2.4 Polymer welding

There are a number of successful techniques used for thermoplastics welding such as hot gas welding, extrusion welding, ultrasonic welding, friction welding, etc. [25]. As the scope of this thesis focusing on friction-based welding, this section will mainly review the literatures relating to this technique only.

Despite friction-based welding such as friction stir welding or ultrasonic welding were very successful for metals, there are some limitations for plastic welding that is difficult to overcome such as [25, 26]: 1) Low welding speed 2) Insufficient heat input due to very low thermal conductivity and inadequate friction energy of lubricous polymer 3) Non-uniform weld bead   4) Uneven polymer mixing   5) Ejection of melted thermoplastic from the weld region. Furthermore, there are additional considerations when welding thermoplastic composites including fiber breaking and distortion of fiber elements [27].

Friction stir welding technique is potentially applicable to weld polymeric materials such as PP, HDPE and UHMW [26]. Kiss and Czigany [28] have studied the applicability of friction stir welding to join polymeric materials by investigating 15-mm-thick polypropylene sheets. They reported the tensile test results of butt-joint specimens were approximately about 50% of the parent material. The crystallinity of different zones is also investigated by DSC techniques. The thermal analysis results showed that the crystallinity in the seam and seam border line is lower than in the matrix. The reason for the reduced crystallinity is from the rapid cooling of molten material by the heat absorption to the tool. The lower crystallinity causes the embrittlement of the seam resulting in low interfacial boding strength at the matrix-seam interface. The SEM micrograph also showed the difference of fracture surface between the matrix and welded seam.

To overcome the limitations of thermoplastic welding, Tracy Nelson et al. [26] proposed the patented friction stir welding tool with a hot shoe as shown in Fig. 12. This tool was developed to overcome the problems from conventional FSW tools including insufficient frictional energy between shoulder-work-piece and ejection of thermoplastic by rotating shoulder. An electric heater connecting with the hot shoe is used to provide heat input for thermoplastic fusion instead of frictional energy from the shoulder. In this way, the hot shoe also functions to provide forging pressure for thermoplastic consolidation and to retain molten thermoplastic inside the weld region. The joints welded by this tool have very good tensile properties at least 75% of the base polymer.

There are some differences in friction stir welding process between thermoplastics and aluminum [26]. Tilted angle and forging pressure are beneficial for aluminum FSW resulting in enhanced material consolidation and better weld strength. However, such high pressure and large tilted angle can cause polymer expansion and high weld bead after the tool has passed (pressure is removed) due to its viscoelastic property.
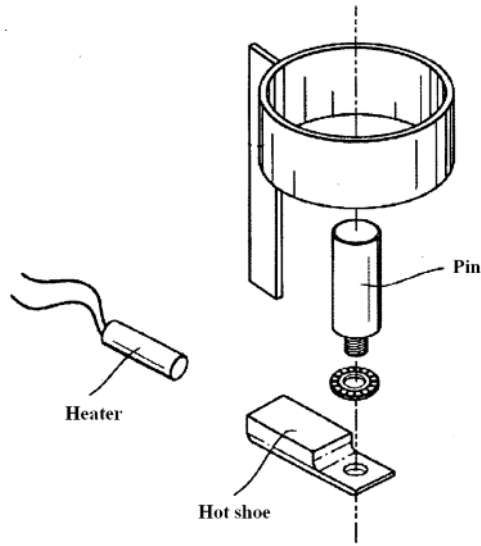
Fig. 12 Friction stir welding tools for thermoplastics developed by Tracy Nelson et al. [26].

Another variant of friction stir welding technique for plastics is called Viblade method [29]. Its tool system consists of oscillating blade and shoulder that are moving in the horizontal direction as shown in Fig.13. The use of the oscillating blade is to overcome an insufficient heat input near the root of the joint because the heat produced by the shoulder cannot reach the bottom of the weld due to very low thermal conductivity of thermoplastics. Viblade method can weld thicker thermoplastic plates comparing with conventional hot gas welding and extrusion welding when the longer blade is used. However, it can weld linear weld line only due to the limitation of blade tool.

a)   b)
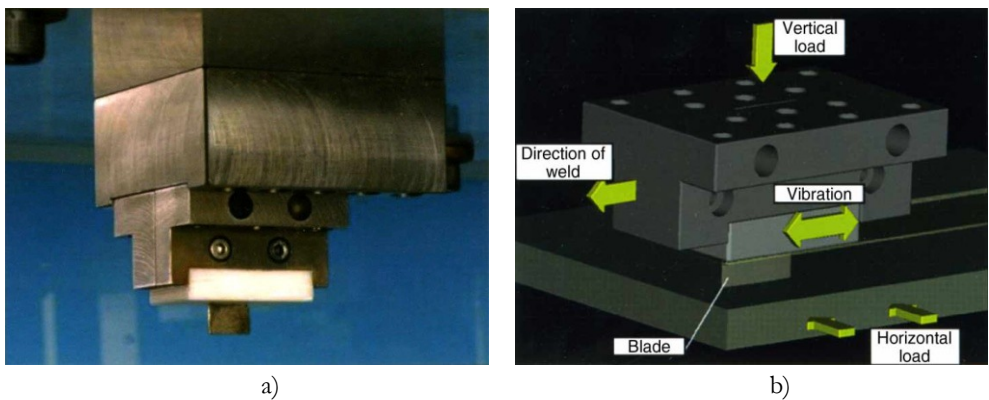
Fig. 13 Viblade welding process invented by TWI. a) Viblade machine b) Description of Viblade process. [29].

2.5 Metal-polymer hybrid welding

Hybrid structures such as metals-thermoplastics or metals-reinforced polymers are increasingly important in the near future innovations. In modern automobile bodies, the material trimming and the replacement of steel to lightweight materials are emerging as the key development in automobile technologies. In addition, the research communities are also interested in combining lightweight alloys to engineering polymers such as CFRP or GFRP for further weight reduction of the structures. However, due to the large dissimilarities between metals and polymers, the sound joining of these materials is difficult to achieve.

Despite the achievement of thermoplastics welding in industrial applications, metal-polymer welding is still a developing method so far due to the differences between metal and polymer properties [3]. As mentioned in chapter 1, there is a large difference in surface energy between metals and polymers which affects the adhesive bonding at interfaces of these two materials. In addition, they also have the dissimilarity structures. Metals have crystalline structures with very high cohesive energy while polymers have long chain molecules with the weak secondary forces in between. When embedded in polymers, metals tend to form round clusters instead of mixing [30] resulting in low solubility of metals in polymers. Degradation of polymers is significantly important especially in metals-polymers joining by welding method. The reasons are from high melting point or high plasticizing temperature of metals which are normally above the degradation temperature of polymers. It can result in lower molecular weight or breakage of polymeric molecules.

One alternative joining method that is successfully used to join metals to composites is friction spot joining (FSpJ) [31]. The principles of FSpJ are developed based on refill-FSSW technique invented by GKSS and shown in Fig.14. Magnesium alloys AZ31 with the thickness of 2 mm were joined to eight-millimeter PPS-CF and PPS-GF. Amancio-Filho et al. reported the results that the shear strength of FSpJ joints is comparable or superior with those reported in the literatures. The failure modes of FSpJ joints can be seen into two categories. At the central region beneath the pin, cohesive fracture can be seen by the adhesion of fiber and polymer matrix to Mg AZ31 plate. Outside the central region, shear mode fracture took place which can be seen from smooth Mg AZ31 plate without the attachment of polymer matrix or fiber. The fracture surfaces of FSpJ joints can be seen in Fig.15.
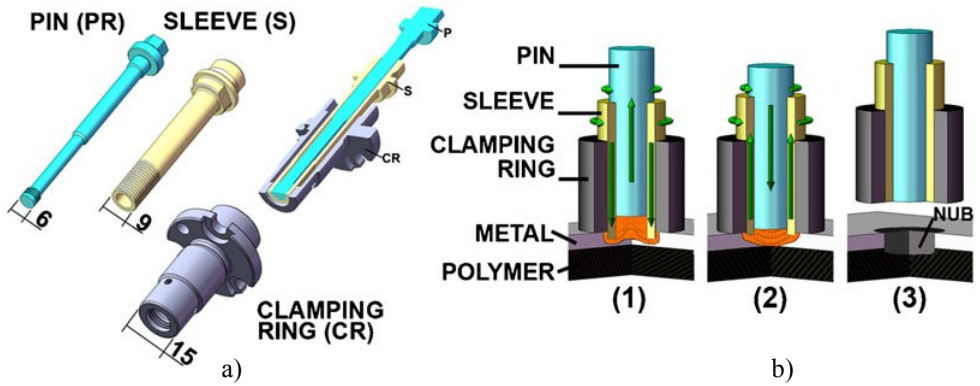
Fig. 14 Schematic showing the principle of friction spot joining welding: Friction spot joining tool assembly b) An illustration of friction spot joining welding process [31].
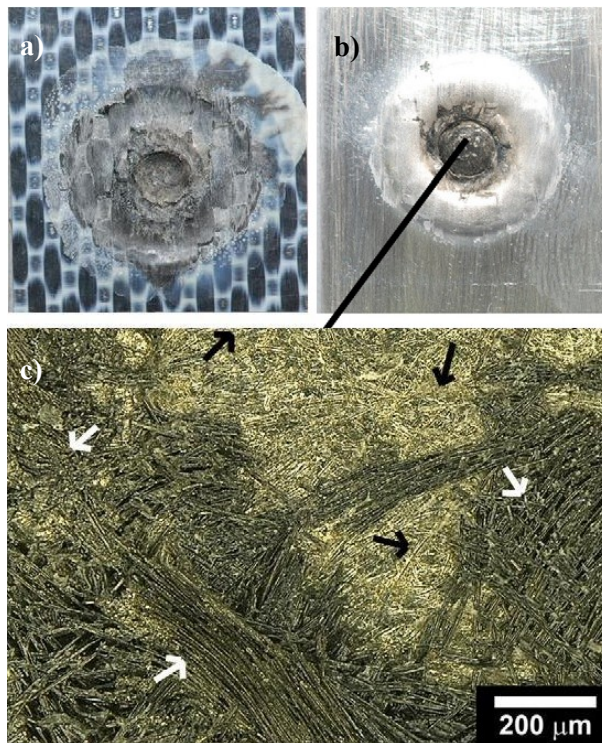

Fig. 15 Fracture surface of AZ31/carbon fiber-reinforced PPS friction spot joining joint. a) PPS-CF plate b) Mg AZ31 plate c) Micrograph showing the central region of spot joint on AZ31 surface [31].

Ultrasonic welding is one of the welding methods that can achieve high quality metal-polymer hybrid joints [32, 33]. A group of researchers at University of Kaiserslautern, Germany reported that the ultrasonic metal welding technique can achieve the highest tensile shear strengths of 23 MPa and 31.5 MPa for AlMg3/Glass-PA12 and AA5754/CF-PA66 respectively. They claimed that the achieved tensile shear strength by ultrasonic metal welding is comparable to those joined by adhesive bonding [32]. The shear strength of joints welded by ultrasonic metal welding is dependent on the level of direct contact between fibers and the metal sheet. As can be seen in Fig. 16, the intimate contact between aluminum alloy and fibers can result in intermolecular bonding and mechanical locking between metal and fibers. At the highest tensile shear strength, the polymer matrix has left the interface between metal and fibers, the direct contact between metal and fibers does develop which enhances the tensile shear strength of hybrid joints.
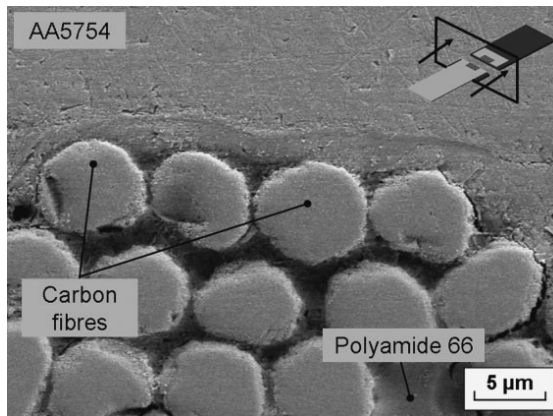
Fig. 16 Schematic showing SEM micrograph of Al/CF-PA66 composite joint welded by ultrasonic metal welding process [33].

2.6 Summary

In order to achieve sound joining by FSW, tool geometries, welding parameters including rotation speed, welding speed and tilt angle should be considered. Whilst large tilt angle promotes material mixing and enhances material consolidation, it may cause material eruption in case of metal-polymer welding due to viscoelastic property of polymer. According to literatures, friction stir spot welding has high possibility to join metal-polymer hybrid structures; however, it is also beneficial to use stitch welding which has the weld length in between ordinary FSW and FSSW in the experiment. In addition, the degradation of polymer and lower crystallinity of polymer should be taken into account when friction stir weld metal-polymer due to the large differences in thermophysical properties.

3. EXPERIMENTAL METHODS

Friction stir welding of thermoplastics and thermoplastic composites to aluminum sheets have been carried out at ESAB laboratory in Laxå. Two sets of trials including one preliminary trial and one main trial were performed using ESAB SuperStir™ machine. The details of material specifications, experimental equipments and experimental setup are reported in this chapter. In order to study the quality of FSW joints, mechanical test with a test standard has been done to evaluate the mechanical properties of the joints. The details of mechanical testing machine setup are also reported in this chapter.

This chapter begins with the specification of material properties including mechanical and thermophysical properties. The second part of this chapter illustrates the equipments used in the experiments including welding machine, FSW tools and testing machines. The details of welding variables are reported in the experimental procedures section in this chapter.

3.1 Materials

The materials used in this study were chosen based on automotive industry applications. The typical aluminum sheets for vehicle bodies are based on Al-Mg alloys such as AA5182, AA5754 and Al-Si-Mg alloys such as AA6016 and AA6111. In this study, two grades of aluminum alloys, AA5754 and AA6111, were investigated. Typical physical and mechanical properties of these two aluminum alloys are given in table 3.1 and 3.2 respectively.

For the first trial, both fiber- reinforced polymers and non-reinforced polymers were used as specimens in the study. The types of investigated polymeric materials are Polypropylene (PP), Polyamide-12 (PA-12), Polyethylene terephthalate (PET), Fiber-reinforced polyethylene terephthalate (PET-PET) and Glass-fiber-reinforced polyamide (PA-glass). Typical thermal properties of investigated polymers are shown in table 3.3. It is noted that the properties shown in table 3.1-3.3 are typical properties from material properties tables, there was no material properties characterization in this study.

Table 3.1 Thermophysical properties of aluminum alloys used in this study [34, 35, 36].

Properties	AA5754-H22[34, 35]	AA6111-T4[36]
Liquidus temperature (°C)	642	652
Solidus temperature (°C)	603	582
Thermal conductivity (W/m·K)	138	167

Table 3.2 Typical mechanical properties of aluminum alloys used in this study [34, 35, 36].

Properties	AA5754-H22[34, 35]	AA6111-T4[36]
Young Modulus (GPa)	70	70
Yield strength (MPa)	177	165
Ultimate tensile strength (MPa)	250	295
% Elongation	13.5	26.0

Table 3.3   Physical properties of polymers used in this study [37, 38, 39].

Properties	PP	PA-12	PET	PET-PET	PA-glass
Glass transition temperature (°C)	-10	45	60/80	60/80	45
Melting temperature (°C)	165	184	160/265	160	184
Decomposition temperature (°C)	350	N/A	340	N/A	N/A
Thermal conductivity (W/m·K)	0.22	0.24	0.24	0.24	0.40
Thermal expansion coefficient ($10^{-4} \cdot K^{-1}$)	6.60	N/A	14.40	0.50	0.08

3.2 Experimental Apparatus

The experiments were performed using ESAB SuperStir™ machine at ESAB laboratory in Laxå, Sweden. ESAB SuperStir™ machine is a custom-designed FSW machine that is suited for high volume production. The picture of ESAB SuperStir™ and its clamping system are shown in Fig.17.

a)   b)
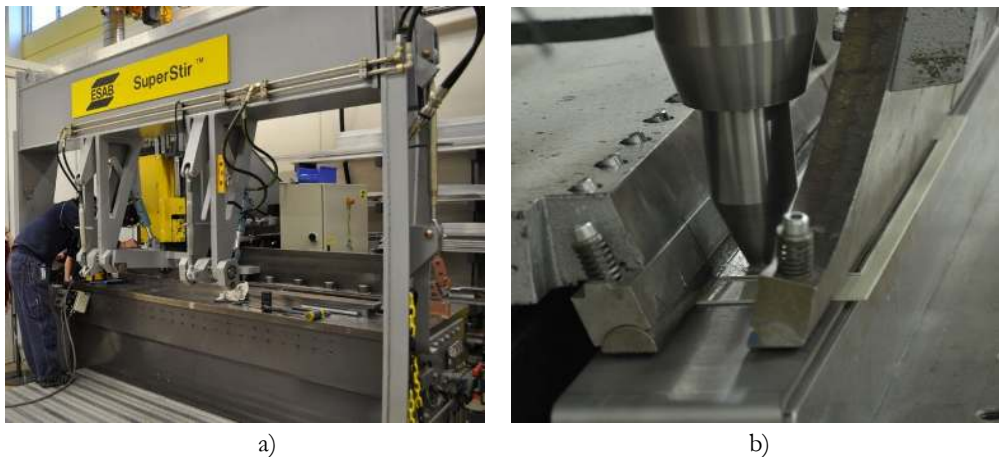
Fig. 17 Schematic showing ESAB SuperStir™ machine. a) ESAB SuperStir™ machine
b) Fixtures and clamping system during FSW operation on ESAB SuperStir™.

3.2.1 Welding Tool

Tool geometries play an important role in thermomechanical characteristics and heat generation in friction stir welding. In the first trial, the specimens were welded by a standard cylindrical threaded pin tool with concave geometry shoulder (Tool E) as shown in Fig.18a. It was made of tool steel with the shoulder diameter and concavity of 15 mm and 7° respectively. The pin dimensions are M6 of diameter and 3.2 mm of length. In the second trial, one additional cylindrical pin tool with scroll groove shoulder (Tool G) was used to investigate the effect of shoulder profile on the quality of hybrid joints. Tool G has the pin dimensions of M6 in diameter and 1.2 mm in length. A groove shoulder diameter is 15 mm and shown in Fig. 18b.

a) b)
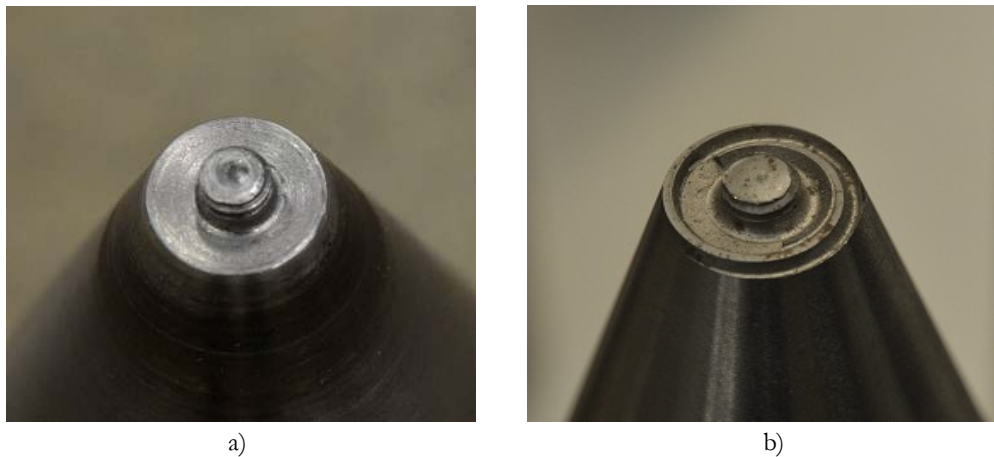
Fig. 18 Schematic showing the welding tools for friction stir lap welding. a) Tool E b) Tool G.

3.3 Experimental Procedures

Two trials were performed in order to study the possibility and conditions of the applicability of friction stir welding for joining various thermoplastics to aluminum alloy sheets. The samples were cut with the dimension of 100×300 mm and assembled in a lap joint configuration. An aluminum alloy sheet was put on the top of a thermoplastic sample on the ESAB SuperStir™ anvil and clamped by two hydraulic fixtures as shown in Fig.17b. Both thermoplastic and aluminum alloy specimens are in the as-received condition without any surface preparation.

The first set of trials investigated the potential material combinations and the effects of welding parameters on the quality of aluminum-thermoplastic hybrid joints. This preliminary study welded various thermoplastics (PP, PA-12, PET) as well as thermoplastic composites (PET-PET, PA-glass) to aluminum alloy sheets by FSW with

Tool E. The parameters under investigation in the first set of trials are material type, sample thickness, rotation speed, tool travel speed and tool plunge depth. The range of parameters for the first trial is summarized in Table 3.4. The results from the first trial were used to determine the potential materials and the test matrix for the second trials.

Table 3.4 Range of welding parameters of each material combination in the first trial

Aluminum	Polymer	Rotation speed (rpm)	Travel speed (rpm)	DTB
AA5754 (1.5)	PP (2.0)	700-2000	10-30	0.1-0.4
AA5754 (2.0)	PP (2.0)	1000-1800	10	0.8
AA6111 (2.0)	PP (2.0)	1600-2000	10	0.7-0.9
AA5754 (1.5)	PA-12 (6.3)	1800	10-20	(-2.2)-(-3.0)
AA5754 (1.5)	PET (2.5)	300-2000	10-20	0.1-0.4
AA5754 (1.5)	PET-PET (2.5)	1000-2000	20-60	0.8
AA5754 (1.5)	PA-glass (0.8×2)	800-1800	20-40	N/A

The preliminary study from the first set of trials indicated that welding parameters especially tool travel speed and welding speed have the great effect on the structure of the joints. The results also showed undesirable structures of the joints such as pores, bending and poor interfacial bonding between metal-polymer. The detail and discussion on the first trial results are given in chapter 4. After analyzing the preliminary study results of the first set of trials, tool geometries and tool tilt angle were added to welding variables under investigation for the second trial. Based on the preliminary study results, the polymers with largest potential to be joined by FSW are two thermoplastics (PP and PA-12) without fibers. In addition, one appropriate aluminum alloy sheet was selected for this joining condition which is AA5754 with thickness of 1.5 mm. Therefore, in the second trial there are two metal-thermoplastic combinations which are AA5754 (1.5) – PP (2.0) and AA5754 (1.5) – PA-12 (2.0) to be performed. Furthermore, Tool E and one additional tool, Tool G, were used for the study of the effect of tool geometries on the weld quality. The range of parameters for the second trial is summarized in the following table.

Table 3.5 Range of welding parameters of each set of experiments in the second trial.

Polymer	Tool	Rotation direction	Rotation speed (rpm)	Travel speed (cm/min)	Tilt angle	DTB
PP	E	CW, CCW	1000-1800	0.5-20	0.5, 2.0	0.2-0.5
PP	G	CCW	1500-1800	3-20	0.5	0.6-1.5
PA-12	G	CCW	1200-1500	3-5	0.5	5.8-5.9

In the second trial, a set of specimens were visually examined. Selected specimens and welding conditions were used for lap shear mechanical testing. In this case, lap shear specimens were made by one aluminum and one thermoplastic sheet with dimension for each of 50×100 mm. The specimens were positioned together with 50×50 mm overlap area by placing the top sheet on the advancing side as shown in Fig.19. Additionally, the specimens were welded with a controlled weld length of 30 mm.
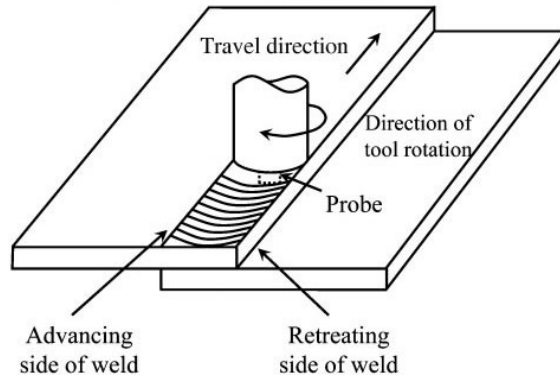
Fig. 19 Schematic showing the lap joint configuration for tensile test [11].

3.4 Tensile test

The lap shear testing was performed using an Instron 4505 testing machine according to ASTM D1002-05 standard [40]. The tested specimens were loaded at a constant displacement speed of 2 mm/min at room temperature. The strain was measured by two extensometers with the length of 50 mm. The load was measured by a 100 kN load cell. The photograph of a specimen under test is shown in Fig. 20

Fig. 20 The photograph showing a specimen in tensile test fixture.

4. RESULTS AND DISCUSSION

As mentioned earlier in chapter 3, there were two sets of trials carried out in this thesis. The first trial was the preliminary study on the effect of major welding parameters for joining of aluminum-thermoplastic by FSW. More detailed experiments to improve the weld quality and insight knowledge regarding the influence of each welding variable have been carried out in the second trial. The results of the entire experiments will be reported and discussed in this chapter.

This chapter includes the results of preliminary study, detailed experiments in the second trial and joint performance analysis by mechanical testing. The weld quality of aluminum-thermoplastic joints was examined by cross-sectional microstructures in terms of pore formation, interfacial bonding, material mixing, chip morphology, sheet rollover and burr formation. The joints characteristics were investigated by electro-deposition and micrographs analysis. The quality of joints in term of weld strength was determined by lap shear test and the results were discussed by fracture mechanics at the end of the chapter.

4.1 First welding trial

A range of thermoplastics and thermoplastics with fibers were joined to aluminum alloy sheets by FSW using Tool E with tilt angle of 2°. There were five kinds of thermoplastics and thermoplastics with fibers including polypropylene (PP), polyamide-12 (PA-12), polyethylene terephthalate (PET), fiber-reinforced polyethylene terephthalate (PET-PET) and fiber-reinforced polyamide (PA-glass) were investigated in the experiments. Two aluminum alloy grades including AA5754 and AA6111 with the thickness of 1.5 and 2.0 mm were chosen to be used. The direction of tool rotation was in a clock-wise direction in the entire experiments. The influence of four main welding variables: type of material, upper plate thickness, rotation speed and travel speed has been studied. The micrographs of welds and the welding parameters used in the first set of trials are summarized in table 4.1. It is noted that advancing side of welds is on the left side of cross-sectional micrographs while retreating side of welds is on the right side.

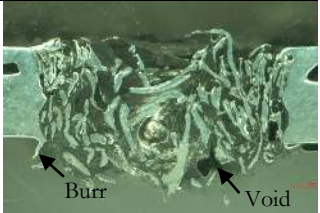Table 4.1a The weld results for each material combination in the first trial
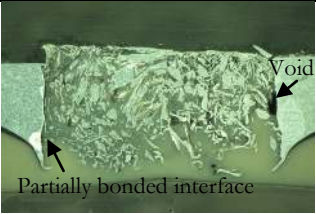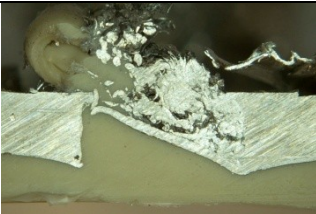
No	Material	Rotation speed (rpm)	Travel speed (rpm)	DTB*	Top view	Cross section
1	AA5754 (1.5)-PP	1800	10	0.1		
2	AA5754 (2.0)-PP	1800	10	0.8		
3	AA6111 (2.0)-PP	1800	10	0.8		
4	AA6111 (2.0)-PP	1600	10	0.7		

Table 4.1b The weld results for each material combination in the first trial
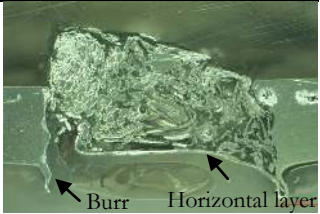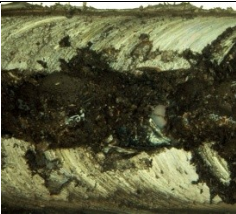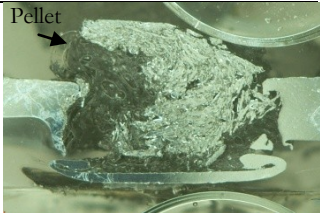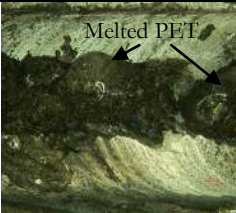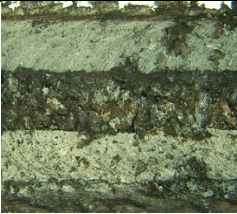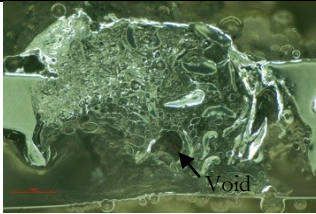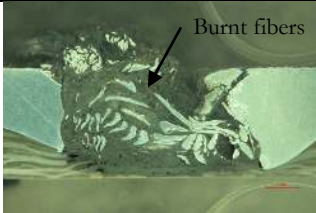
No	Material	Rotation speed (rpm)	Travel speed (rpm)	DTB*	Top view	Cross section
5	AA5754 (1.5)-PA12	1800	10	-2.2		
6	AA5754 (1.5)-PA12	1800	20	-2.2		
7	AA5754 (1.5)-PET	2000	10	0.1		
8	AA5754 (1.5)-PET	1500	20	0.2		

Table 4.1c The weld results for each material combination in the first trial

No	Material	Rotation speed (rpm)	Travel speed (rpm)	DTB*	Top view	Cross section
9	AA5754 (1.5)-PET	1000	20	0.2		
10	AA5754 (1.5)-PET-PET	1000	40	0.8		
11	AA5754 (1.5)-PA-glass	1800	20	N/A		

Note: * - DTB stand for distance to backing of FSW tool

The micrograph analysis of weld cross sections in table 4.1a-4.1c showed that specimens welded by FSW in the first trial contain defects and flaws in almost all specimen samples. However, it is also showed that FSW can possibly be applied to join thermoplastics to aluminum alloy sheets if appropriate welding parameters are used.

4.1.1 Material flow and microstructure

The microstructure of aluminum-thermoplastic welds is asymmetric about the center of weld line. The asymmetric flow is developed around the pin by the deviation in velocity and pressure fields [41]. Fig.21a shows the microstructure of the weld consisting of aluminum chips surrounded by thermoplastic matrix. The direction of molten thermoplastic flow is controlled by threaded pin to flow in vertical direction near the pin towards the shoulder. Voids can be seen at retreating side (right-hand side of cross-sectional micrographs) in case of clock-wise rotation as can be seen from sample 1, 6, 8 and 9. It is evident from Fig.21a that partially bonded interfaces between aluminum parent material (upper plate) and aluminum-thermoplastic composite weldment can be visually seen at some welding parameters.
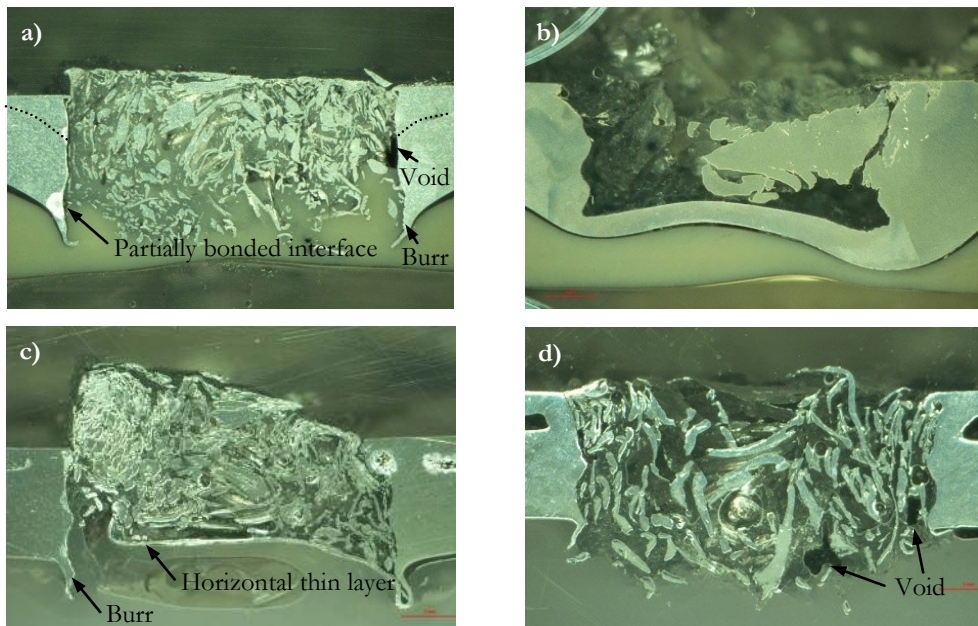

Fig. 21 The micrographs of aluminum-thermoplastic joint cross. a) AA5754 (1.5)-PP joint welded with 1800 rpm, 10 cm/min b) AA5754 (2.0)-PP joint welded with 1800 rpm, 10 cm/min c) AA5754 (1.5)-PA12 joint welded with 1800 rpm, 10 cm/min d) AA5754 (1.5)-PA12 joint welded with 1800 rpm, 20 cm/min

Fig 21c and 21d show the effects of tool travel speed on aluminum chip morphology and existence of horizontal thin layer. It can be seen that low travel speed results in fine aluminum chip weldment compared with higher travel speed. This is associated with metal cutting theory which can be used to explain friction stir welding process [42]. For both FSW and metal cutting process, the term weld pitch, which is the ratio of travel speed to rotation speed, controls chip morphology during the process. For FSW, chip formation morphology changes from continuous to segmented when the weld pitch is increasing. It is comparable to a decreasing in cutting speed causes chip morphology to be changed from continuous to discontinuous in case of machining or metal cutting process.

Horizontal thin layer tends to form when using low travel speed friction stir welding as shown in Fig 21b and 21c. The thickness of upper plate that the rotating tool can be used is associated with tool geometries, tool dimension and tool travel speed [43]. In aluminum-thermoplastic FSW, softening of thermoplastic sheet reduces the upper plate thickness that can be used. The maximum thickness of upper plate that can be used for Tool E is up to 1.5 mm as shown in Fig 21a. An increase in thickness up to 2.0 mm (both AA5754 and AA6111) is not possible for this tool geometry because the tip of the pin cannot plunge into the thermoplastic sheet as can be seen in case of sample 2 and 3 in table 4.1a. However, it is not clear from the first trial results that this horizontal thin layer is influenced by low travel speed or together with high degree of tilt angle. This issue will be investigated further in the second trial.

4.1.2 Defects

The defects found in aluminum-thermoplastic friction stir welding are porosity, surface roughness, flash formation, burr formation, upper plate rollover and thermoplastic eruption. The formation of voids can be seen at the retreating side of welds as shown in Fig 21a, and 21d. This is a result of insufficient material flow near the bottom of the pin due to insufficient heat generation, high weld pitch or large pin diameter [44]. If the generated heat is too low, the molten thermoplastic cannot flow properly to fulfill the weld line behind the tool especially in case of large pin diameter. If too high travel speed were used, the molten thermoplastic will solidify before all spaces are filled. The porosities or voids will form at the retreating side in case of clock-wise rotation direction where the material has inadequate flow.

Burr formation can be observed in several aluminum-thermoplastic combinations: PP, PA-12 and PET which can be seen in Fig.21a-21d. In addition, upper plate rollover (bending) as shown in Fig.21a occurs in case of AA5754-PP welding when using high travel speed. Both burr formation and upper plate rollover are due to soften thermoplastic sheet and high welding forces exerting on the work-piece. During the

process, local frictional heat at the contact between shoulder and work-piece surfaces causes the adjoining thermoplastic to be softened. This leads to deformation of the upper work-piece when the rotating tool exerts force on the weld due to softening of underlying support plate. Welding forces are associated with the degree of tilt angle, rotation speed and travel speed [41]. The produced forging pressure on the weld increases by increasing tilt angle or travel speed. However, insufficient welding forces leads to low heat generation and poor joint quality. Therefore, it is necessary to optimize the degree of tilt angle by considering tool geometries, thermophysical properties of thermoplastics and welding parameters.

Fig 22a and 22b present the surface appearance of AA5754-PP and AA5754-PET showing the excess flash forms on the work-piece surfaces. This corresponds with surface overheating due to excess frictional heat between the shoulder and the work-piece [44]. In addition, the large tool plunge depth (small distance to backing) also increases the size of flash on the surface.
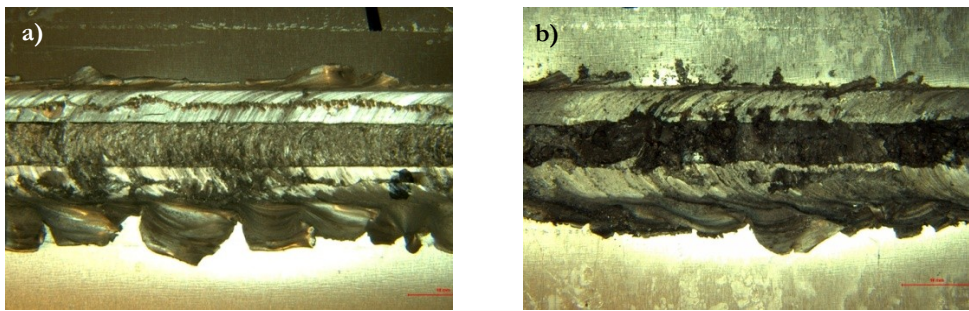
Fig. 22 Photographs of aluminum-thermoplastic joint surface appearances. a) AA5754-PP joint welded with 1800 rpm, 10 cm/min b) AA5754-PET joint welded with 2000 rpm, 10 cm/min

Eruption of thermoplastics can be found in some specimens when welding with high rotation speed and low travel speed as shown in Fig 23a-23b. Small weld pitch, low ratio of travel speed to rotation speed, leads to an increase in peak temperature during friction stir welding due to high heat generation rate per unit weld length. The occurrence of thermoplastic eruption is visibly seen in case of Al-PET welding. The cross section of sample 7, 8 and 9 in table 4.1 show the eruption of PET and regular melted PET pellets in wide trench along the weld line. Typically, viscoelastic property of polymers causes high weld bead due to polymer expansion after the tool pressure was removed as shown in Fig. 21c. High weld bead tends to form when using high welding force condition such as small distance to backing (DTB). In addition, low melting temperature and high coefficient of thermal expansion of thermoplastics will further increase the level of volume expansion as can be seen in case of thermoplastic eruption.

4.1.3 Polypropylene (PP)

The micrographs in Fig 21a-21b present microstructure of welds made by AA5754-PP combination. The results showed that AA5754-PP combination had good weldability using friction stir welding. By lowering travel speed and increasing rotation speed, the mixing of aluminum and PP is promising with a good surface finish. The best obtainable result of AA5754 (1.5)-PP weld was achieved with rotation speed of 1800 rpm and travel speed of 10 cm/min as shown in Fig.21a. However, burr and upper plate bending are found in AA5754-PP joint cross sections when using high travel speed FSW.

4.1.4 Polyamide-12 (PA-12)

A good mixing of aluminum and thermoplastic can be seen from the micrograph in Fig.21c and 21d for AA5754-PA-12 combination. This material combination has a good weldability in term of material mixing, small size of burr and low distortion. However, porosities and voids can be seen across the weldment when joining with high weld pitch as can be seen in Fig. 21d. There was no PA-12 eruption or melted pellet found in the experiments. It is also noticed that flash can be seen on the surface of the specimens.

4.1.5 Polyethylene terephthalate (PET)

Fig 23a shows the cross section of AA5754-PET weld containing melted PET pellets and high weld bead. According to table 3.3, the coefficient of thermal expansion of PET is at least two times higher than other thermoplastics. It results in additional volume expansion when PET is melted during friction stir welding. In addition, there was smoke and burning of PET when using low weld pitch. On the other hand, while using large weld pitch, lack of material filling and wide trench become two main problems instead of PET eruption. Micrographs of Al-PET cross sections also showed that trapped bubbles inside weldment is significantly found in Al-PET cross sections compared to other material combinations as shown in Fig 23b.
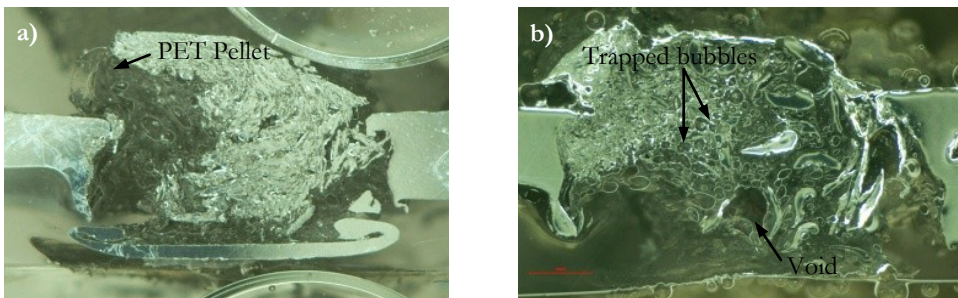

Fig. 23 Photographs of AA5754-PET joint cross sections and surface appearance. a) Joint welded with 1500 rpm, 20 cm/min b) surface appearance of joint welded by 1500 rpm, 20 cm/min.

4.1.6 Fiber-reinforced thermoplastics

Two thermoplastics with fibers, fiber-reinforced polyethylene terephthalate (PET-PET) and glass-fiber-reinforced polyamide (PA-glass), were joined to aluminum alloy sheets in the first trial. However, for aluminum-thermoplastic with fibers FSW, fiber breakage and distortion of fibers in polymer-matrix composites can be seen in Fig.24a and 24b. In addition, there was burning of fibers and polymer matrix during friction stir welding due to high friction coefficient between the rotating tool and fiber elements especially joining of AA5754-PA-glass. This can be visually seen as the dark region in Fig.24b. Additionally, glass fibers also hinder thermoplastic upward flow to fill in the joint which results in wide trench and longitudinal void along the weld line as seen in Fig 24a.
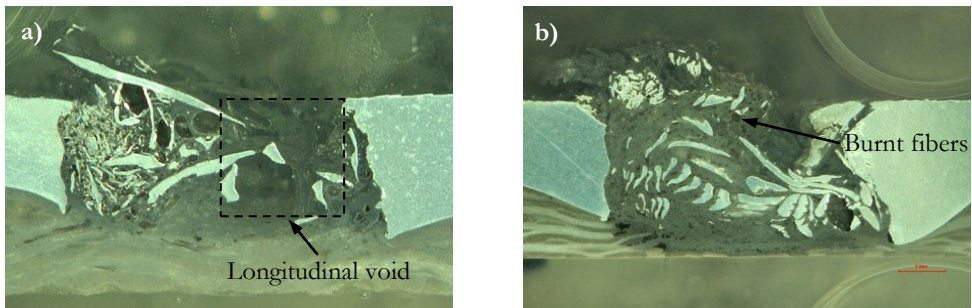
Fig. 24 The macrographs of aluminum-thermoplastic with fibers joint cross sections. a) AA5754-PET-PET joint welded with 1000 rpm, 40 cm/min b) AA5754-PA-glass joint welded with 1800 rpm, 20 cm/min.

The best obtainable welds in the first set of trials as well as welding parameters are summarized in Table 4.2. The values of welding parameters together with the analysis will be used as the guideline for a design of test matrix of the second trial which is summarized in Table 3.5 in the previous chapter.

Table 4.2 The obtainable welding results for each material combination in the first trial

Aluminum	Polymer	Rotation speed (rpm)	Travel speed (rpm)
AA5754 (1.5)	PP (2.0)	1800	10
AA5754 (1.5)	PA-12 (6.3)	1800	20
AA5754 (1.5)	PET (2.5)	1500	20
AA5754 (1.5)	PET-PET (2.5)	1000	40
AA5754 (1.5)	PA-glass (0.8×2)	1800	20

4.2 Summary from the first trial

Welding parameters including rotation speed and travel speed play the important role in aluminum-thermoplastic friction stir welding. More detailed investigation of the influences of these parameters will be systematically investigated in the second trial. In order to improve the aluminum-thermoplastic joint quality especially burr formation and upper plate bending, the effects of tilt angle will be studied in the second trial.

According to micrographic analyses, PET, Fiber-reinforced PET (PET-PET) and Glass-fiber-reinforced PA (PA-glass) are excluded in the test matrix of the second trial due to physical properties limitation. The materials under investigation in the second trial are PP and PA-12 only. The maximum pin length of existing tools at ESAB laboratory is only 3.2 mm (Tool E); therefore, only AA5754 with thickness of 1.5 mm will be used in the second trial.

The best obtainable welding parameters in table 4.2 will be used as the guideline for welding parameters selection in the second trial. The aim for a design of test matrix in the second trial is to minimize pore and defect formation. By doing this, loss of aluminum chips during FSW should be reduced and the term weld pitch should be closely considered.

4.3 Second welding trial

Apart from the basic factors that have been studied in the first trial, more detailed experiments on the influences of welding parameters including tool rotational direction, tool tilt angle and tool geometries have additionally been investigated. The causes of defect formation such as non-optimum welding parameters and abnormal material flow characteristics were analyzed and discussed. The agreement of the weld quality was clarified by the mechanical test at the end of the section. The welding parameters and the micrographs of specimen cross sections are summarized in the following tables

Table 5.1a Welding parameters of each experiment in the second trial.
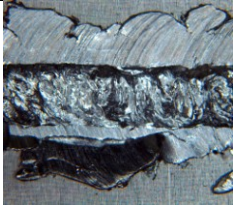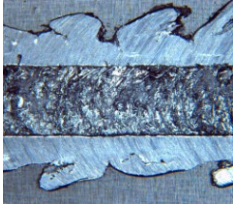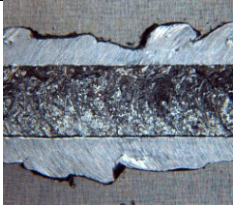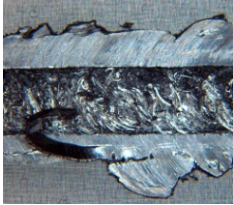
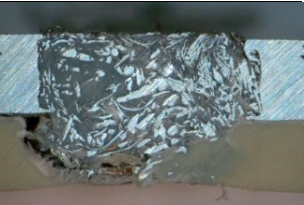| Sample	Polymer	Tool	Rotation direction	Rotation speed (rpm)	Travel speed (cm/min)	Tilt angle	DTB	Top view	Cross section
1	PP	E	CCW	1800	5	2	0.5		
2	PP	E	CW	1800	5	2	0.5		
3	PP	E	CW	1800	5	0.5	0.5		
4	PP	E	CCW	1800	5	0.5	0.5		

Table 5.1b Welding parameters of each experiment in the second trial.
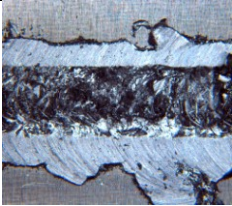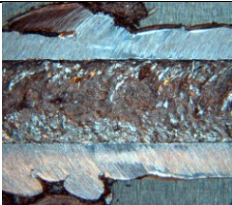
Sample	Polymer	Tool	Rotation direction	Rotation speed (rpm)	Travel speed (cm/min)	Tilt angle	DTB	Top view	Cross section
5	PP	E	CW	1800	20	0.5	0.5		
6	PP	E	CW	1000	5	0.5	0.5		
7	PP	E	CW	1000	20	0.5	0.5		
8	PP	E	CW	1800	5	0.5	0.2		

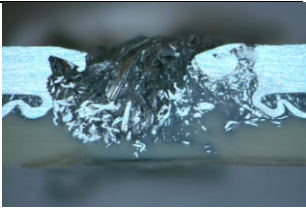Table 5.1c Welding parameters of each experiment in the second trial.
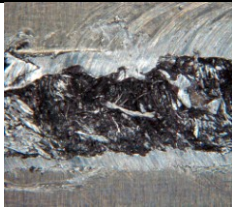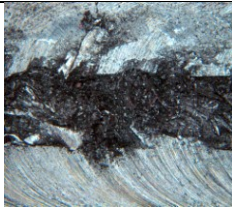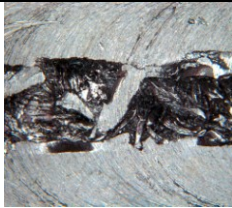
Sample	Polymer	Tool	Rotation direction	Rotation speed (rpm)	Travel speed (cm/min)	Tilt angle	DTB	Top view	Cross section
9	PP	G	CCW	1800	5	0.5	1.6		
10	PP	G	CCW	1800	5	0.5	1.4		
11	PP	G	CCW	1800	5	0.5	1.5		
12	PP	G	CCW	1500	5	0.5	1.5		

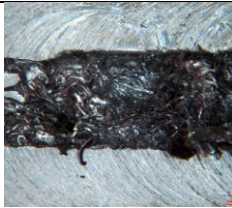Table 5.1d Welding parameters of each experiment in the second trial.
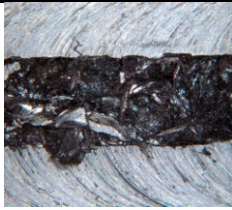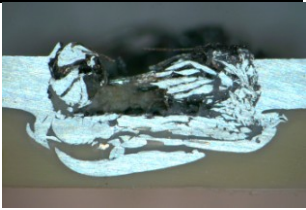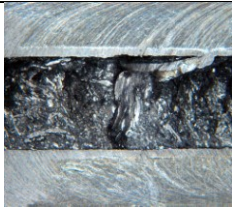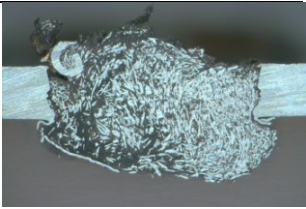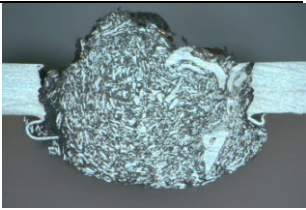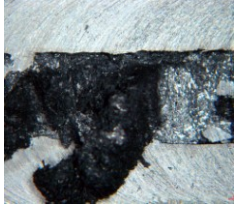
Sample	Polymer	Tool	Rotation direction	Rotation speed (rpm)	Travel speed (cm/min)	Tilt angle	DTB	Top view	Cross section
13	PP	G	CCW	1500	20	0.5	1.5		
14	PP	G	CCW	1500	3	0.5	1.5		
15	PA-12	G	CCW	1500	5	0.5	5.8		
16	PA-12	G	CCW	1500	3	0.5	5.8		

Table 5.1e Welding parameters of each experiment in the second trial.

Sample	Polymer	Tool	Rotation direction	Rotation speed (rpm)	Travel speed (cm/min)	Tilt angle	DTB	Top view	Cross section
17	PA-12	G	CCW	1200	3	0.5	5.8		

4.4 Weld formation and material flow

The welding results of the second trial revealed that there was a significant improvement on weld quality in terms of material mixing and weld defects compared with the first trial. A promising mixing between aluminum and thermoplastic was obtained as shown in Fig 25a and 25b. A small size of voids can be found at retreating side of weldment for AA5754 and PP combination, while void-free weld was obtained when AA5754 and PA-12 combination was joined as shown in Fig 25b.
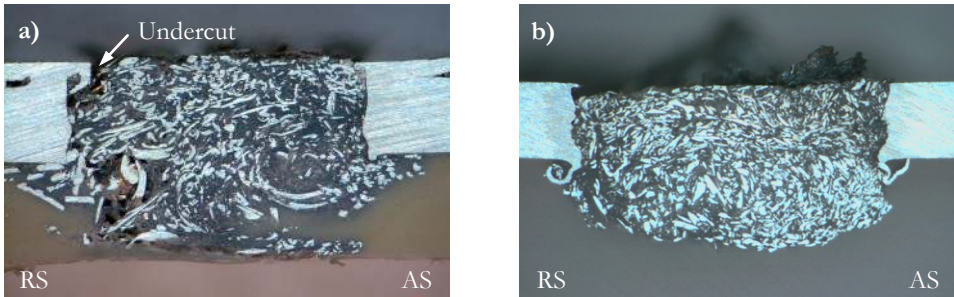

Fig. 25 The micrographs of aluminum-thermoplastic joint cross sections. a) AA5754-PP (1800 rpm, 5 cm/min, 0.5°, CCW, Tool E) b) AA5754-PA-12 (1200 rpm, 3 cm/min, 0.5°, CCW, Tool G)

Fig 26a-26d show the cross sections of AA5754-PP welds at different degree of tilt angle in both rotational direction. It is evident from the micrographs that asymmetric microstructure of welds was developed about the weld centerline. The friction stir weldment consists of aluminum fragments (chips) surrounded by thermoplastic matrix. Voids can be seen at retreating side of weldment while void-free can be obtained at advancing side for both rotational direction. Material flow characteristic is considered to be an important factor that influences the defect formation and the quality of welds [45]. During friction stir welding, the welding parameters including rotation speed, travel speed, axial force, tool tilt angle and tool geometries control the motion of material inside the weld nugget. It is also noticed from the micrographs that flash is formed on the work-piece top surface in all specimens in Fig 26a-26d.

Voids or groove-like defect in Fig. 26b-26d are caused by an insufficient material filling up the weld cavity beneath the shoulder. It occurs by the consequences of material loss due to ejected aluminum chips/flash formation and lack of adequate material flow inside the weld cavity. Fig. 26a and 26c also show that the size of voids reduces as the degree of tilt angle increases in case of counterclockwise rotational direction. On the contrary, an increase of tilt angle leads to a greater size of voids in case of clockwise

rotational direction. The different material flow characteristic is believed to be the reason for the positive and negative effect when the degree of tilt angle was changed.
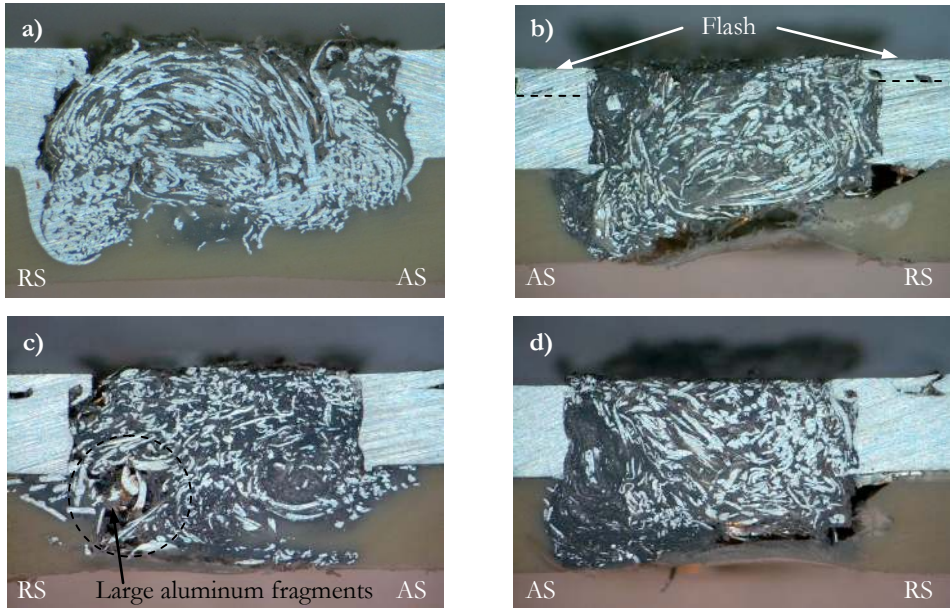
Fig. 26 The micrographs of AA5754-PP joint cross sections. a) 1800 rpm, 5 cm/min, 2°, CCW b) 1800 rpm, 5 cm/min, 2°, CW c) 1800 rpm, 5 cm/min, 0.5°, CCW d) 1800 rpm, 5 cm/min, 0.5°, CW.
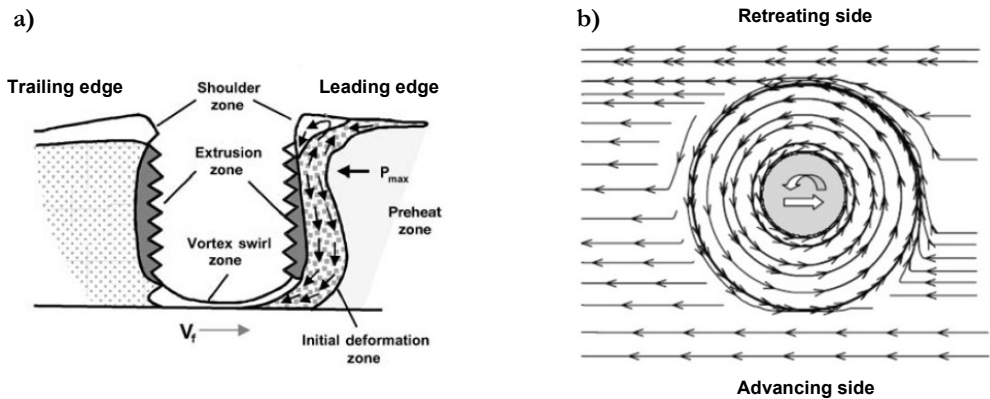

Fig. 27 a) Schematic of friction stir tool geometries in longitudinal view showing the leading and trailing edge [46]. b) Stream line showing the asymmetric material flow around the rotating tool during the translation (horizontal view during CCW rotation) [47].

4.4.1 Material flow in different rotational direction

The micrographs in Fig 26a-26d presented a large difference in material flow characteristic between specimens welded by counterclockwise and clockwise rotational direction. It can be observed from the micrographs that a large worm-hole defect is formed in the weldment of specimens welded using CW tool rotational direction. While using CCW tool rotational direction, a smaller size of voids or even void-free can be obtained in the weldment.

When the tool rotates in CCW rotational direction, the incoming material from the leading edge is transported to the trailing edge by so-called pin-driven material flow as schematically illustrated in Fig 27a. The motion of this material is driven by the pin threads which push the deformed material downward to the pin bottom in the thickness direction. The resulting equivalent amount of material is driven by this deformed material to flow upwards somewhat farther away [6]. The stream trace in Fig 27b indicates that the material in the leading edge is intensely transported to the weld cavity behind the tool mainly through the retreating side [47]. In the weld cavity, during the material is upwardly transported from retreating to advancing side, the relatively cooler base material resists the motion of transported material to reach the advancing side. If this resistance is high or the pressure underneath the shoulder is low, the material will tend to flow out at the channel between the shoulder and the workpiece, the flash is formed on the surface at the retreating side [45].

The microstructure investigation of Fig 26c show that the relatively large size of aluminum fragments are obviously found in the region of void formation compared to the void-free region in which contains finer aluminum fragments. The presence of the large fragments at the lower retreating side leads to a lack of adequate material flow inside this region. This consequently causes the stagnant zone where the flow of the transferred material is not capable to pass the region; the voids are subsequently formed due to an insufficient material filling. The occurrence of heterogeneous size of aluminum fragments is stimulated by the non-uniform temperature at the different position of pin threads. While the upper zone near the shoulder has significant higher temperature by the interaction of shoulder and work-piece surface, the lower zone near the pin bottom has relatively low temperature due to only viscous heat is generated. As a result, the different size of aluminum chip is formed. The large size of aluminum fragments found in the stagnant zone may result from the chip formation at the bottom of the pin where the temperature is lowest.

The reason that coarse aluminum fragments were found in the lower retreating side region is due to the fact that aluminum chips in front of the tool are picked up by the rotating tool and transferred predominately via the retreating side to the weld cavity. As

shown in Fig 27a and 27b, the pin threads transfers the incoming material (aluminum chips) by superposition of vertical flow and redial flow mainly around the pin in the retreating side. However, due to the large size of fragments and weak circulation, the aluminum fragments become trapped in this region; an insufficient of material flow subsequently occurs which leads to void formation in the region.

Fig 26c and 26d show the influences of tool rotational direction when the direction was changed from CCW to CW rotational direction. It is obviously seen from the micrographs that the size of voids at the retreating side is significantly larger in the joint welded using CW rotational direction compared to the joint welded using opposite rotational direction. By using the same pin thread (right-hand thread), the deformed material in front of the tool is conveyed in upward direction towards the shoulder as can be seen in Fig 28. The deformed material will consequently leave the weld cavity at the leading edge in front of the tool. A huge loss of material due to ejected aluminum fragments and flash formation leads to an insufficient amount of material to fill up the weld cavity, the large size of voids will be formed.
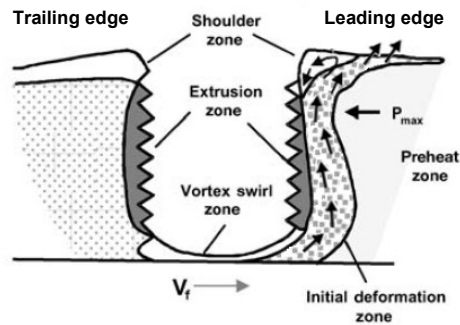
Fig. 28 Schematic of friction stir tool geometries in longitudinal view showing the leading and trailing edge when using the tool rotates in clockwise direction [46].

In the following section, the mechanism of joining and weld defect formation that are influenced by welding parameters will be illustrated. The heat generation and aluminum chip formation morphology are significantly affected by so-called weld pitch as previously mentioned in section 4.1. It is noticed from the first trial that weld defects such as voids and flash are caused by non-optimum friction stir welding conditions especially rotation speed and welding speed. However, sheet rollover and burr formation have not yet been classified in the previous section.

4.5 Effects of tool tilt angle and geometries

Fig 26a and 26c, 26b and 26d present the role of tool tilt angle on the size of voids formed in the weldments of AA5754-PP combination. It can be observed from the cross sections that there are positive and negative effects when the tilt angle was changed from 2° to 0.5°. For the specimens welded using CCW rotational direction, an increase of tilt angle promotes a more promising mixing and defect formation improvement in the weldments. While using CW rotational direction, a larger degree of tilt angle increases the size of voids or worm-hole at the retreating side of the welds.
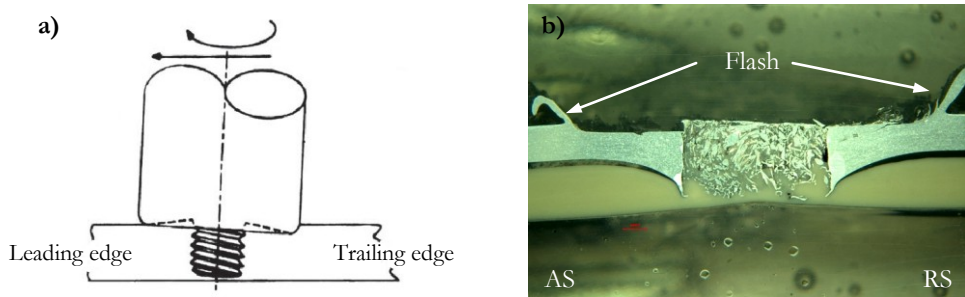

Fig. 29 a) Schematic showing the tool interaction to the work-piece at the leading edge and trailing edge [48] b) The cross sections of joint welded with a high degree of tilt angle (2°) showing a large mass of flash at the retreating side (1800 rpm, 10 cm/min, , CW).

The tool tilt angle is an essential factor that controls the heat generation rate and the material flow inside the weld cavity. During the process, the heat generation rate as well as the peak temperature increase with the degree of tilt angle while other welding parameters are kept constant. The resulting flow of material is subsequently enhanced due to an easing movement of deformed material at elevated temperature. Furthermore, a small degree of tilt angle results in an increase in contact pressure between the tool and the work-piece especially in the trailing edge [45]. Consequently, a more intense of material flow at the back of the tool is developed due to enhanced material extrusion near the pin end and sub-surface material flow beneath the shoulder [45, 48].

In case of CCW rotational direction, a change of tilt angle from 2° to 0.5° promotes the circulation of material inside the weld cavity. A thread-driven action which transfers the deformed material in vertical direction is enhanced by an increase in tilt angle. The better flow of material inside the weld cavity is subsequently obtained. A promising mixing and resulting void-free welds will possibly be achieved in the weldment.

On the other hand, in case of CW rotational direction, an increase in thread-driven action due to a large tool tilt angle gives the negative effect to the quality of welds. Both

thread-driven action and easing material flow inside the weld cavity increase a loss of aluminum fragments though the leading edge in front of the tool as shown in Fig 28. An insufficient amount of material to fill up the weld cavity will become a significant problem which results in a larger void formation in the weldment as the one in Fig 26b.

The results from the experiments also showed that a high degree of tilt angle promotes an excessive flash formation formed on the work-piece top surfaces. It can be seen from Fig. 29b that when a high tilt angle of 2° was used, a large mass of flash is generated in both the advancing and retreating side. However, the size of flash formed on the retreating side is significantly greater than those formed on the advancing side. The description of the origin of flash formation has briefly discussed in the previous section. In this section, the more detailed description of a role of tilt angle on flash formation will be further illustrated.
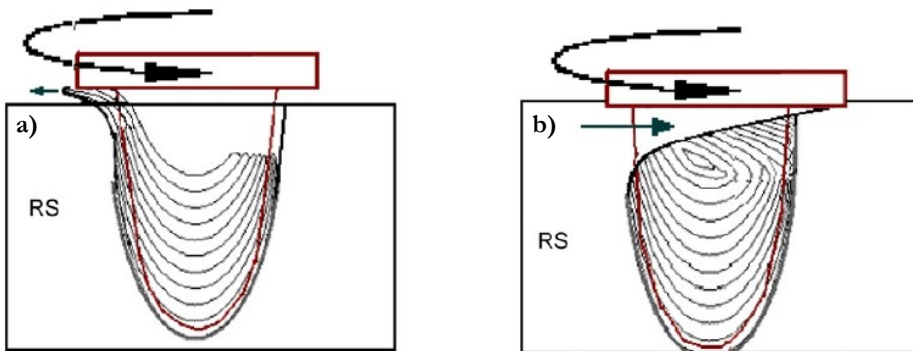

Fig. 30 Material flow inside the weld cavity at the various shoulder interaction [45] a) Flash formed on the work-piece top surface b) Material flow under the pin-driven and shoulder-driven flow without flash.

Tool tilt angle plays an important role on contact pressure between the shoulder and work-piece top surface. A proper degree of tilt angle can generate sufficient amount of heat and hydrostatic pressure for producing a defect-free welds [45]. However, a large degree of tilt angle tends to generate a great deal of contact pressure due to confinement of deformed material within the weld cavity [45]. This results in an excess heat generation and flash formation which is generally formed at the retreating side of weldment as schematically shown in Fig 30a. The flash formation is a result of an escape of transferred material from the weld cavity through the gap between the shoulder and the work-piece surface. The tradeoff between void formation and flash formation should be compromised by considering a well-adjusted tilt angle coupling with appropriate welding conditions during the process.

Another way to reduce flash formation on the surface is to use different shoulder geometries for friction stir welding tool. Fig. 30a-30b present the joint welded using scroll shoulder tool (Tool G) which delivers a flash-free weld with low level of void formation. The main advantage of replacement of the concave tool (Tool E) by the scroll shoulder tool is an elimination of flash by shearing of material on the work-piece top surface. It is also noticed that the tool is normal to the work-piece surface (zero-tilt angle) when the scroll shoulder tool is used in friction stir welding operation. This can drastically reduce the axial load as well as contact pressure that the tool exerts on the work-piece surface, the flash and sheet roll over are then eliminated.
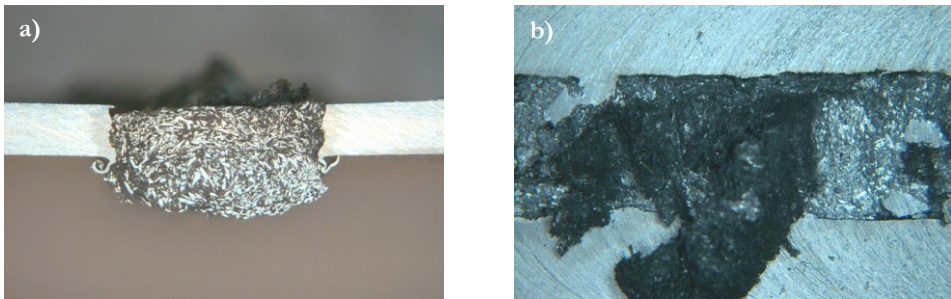

Fig. 30 a) The micrographs of AA5754-PA12 joint cross sections (1200 rpm, 3 cm/min, 0.5°, CCW) b) The photographs of surface appearance of the same joint as in Fig 30a.

4.6 Effects of travel speed and rotation speed

Fig. 31a-31d show the upper sheet rollover (bending) and burr formation of the welds are influenced by an excess travel speed. It is evident from the micrographs that a promising cross section (Fig. 31a, 31c) in terms of burr-free and non-distortion sheet was obtained using low travel speed. By increasing the travel speed from 5 to 10 cm/min, burr and sheet rollover were found in the welds as shown in Fig. 31b.

The concept of friction stir welding process can be regarded as equivalent to the mechanisms of milling operation in typical metal cutting processes [49]. Fig 32 schematically presents the analogy in terminology between so-called advancing side and retreating side in FSW and up-milling and down-milling in plain milling operation. The shear surface around FSW tool and the metal cutting shear plain in milling operation is comparable with each other. The results from the experiments demonstrated that during aluminum-thermoplastic FSW, there were dramatic changes in operation from milling-like FSW (Fig. 31a, 31c) to milling-shearing-like FSW (Fig. 31b, 31d) when the travel speed increases. The results of micrographic analyses of specimen in Fig. 31b presented the grain shape of aluminum alloy near the tip is elongate and different from the grain shape of parent material somewhat far away as can be seen in Fig.33a-33b.
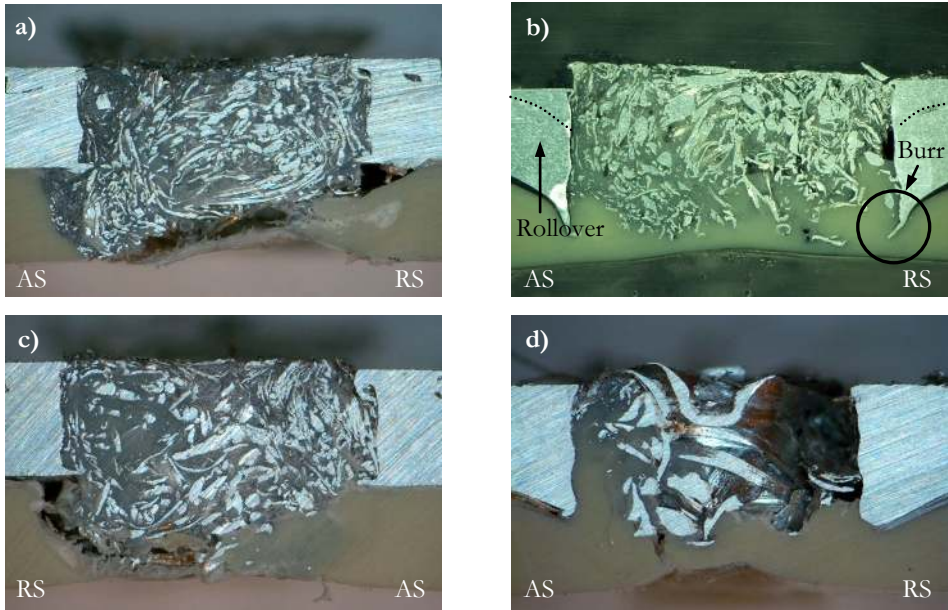
Fig. 31 The micrographs of AA5754-PP joint cross sections. a) 1800 rpm, 5 cm/min, 2°, CW b) 1800 rpm, 10 cm/min, 2°, CW. c) 1000 rpm, 5 cm/min, 0.5°, CW d) 1000 rpm, 20 cm/min, 0.5°, CW
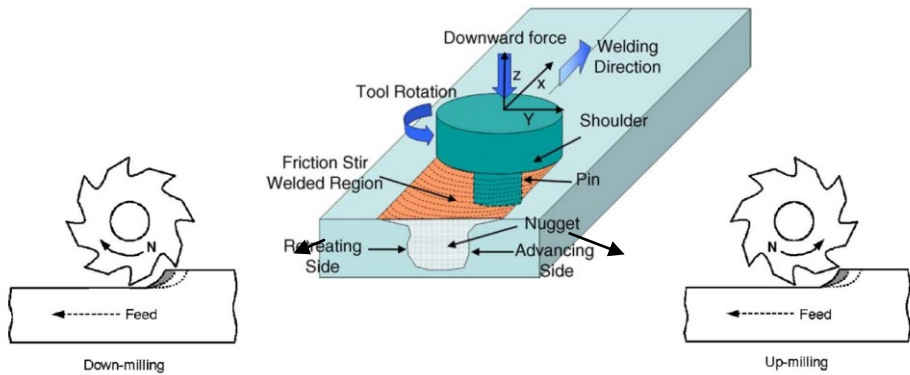

Fig. 32 Comparison of the terminology in FSW and typical milling operation [9].
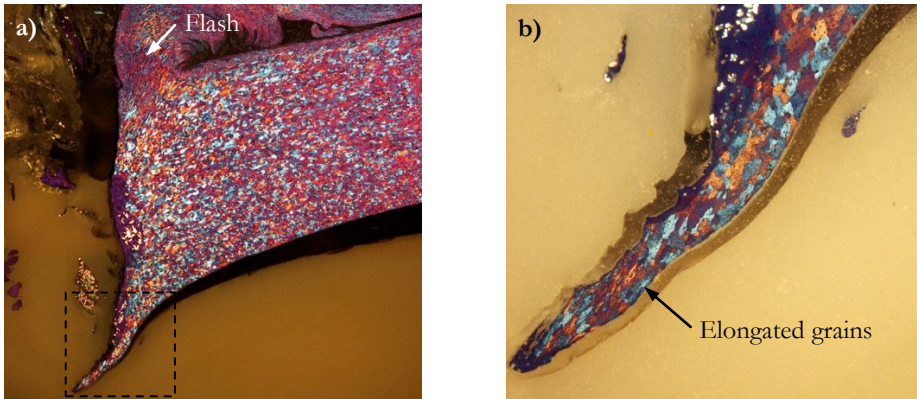
Fig. 33 a) Microstructure of AA5754-PP joint cross sections (1800 rpm, 10 cm/min, 2°, CW)
b) Elongated grains of burr formed in AA5754-PP joint (1800 rpm, 10 cm/min, 2°, CW)

At a high travel speed, the rotating threaded pin is unable to perform adequate cutting action for incoming aluminum alloy work-piece. This results in insufficient material removal from the cutting zone which leads to an increase of cutting forces and the distortion of aluminum alloy sheet. The milling-like FSW then become milling-shearing-like FSW. The deformation of grains from equiaxed to elongated grains in Fig.33b results from shearing of aluminum alloy sheet in the thickness direction by mechanical punching during the tool transverses along the weld line. The shearing of aluminum sheet during FSW can be regarded as the process of sheet metal cutting by shearing processes as shown in Fig. 34a. The mechanism of burr formation and upper sheet rollover of the welds at high travel speed will be discussed by the theory of metal trimming process.
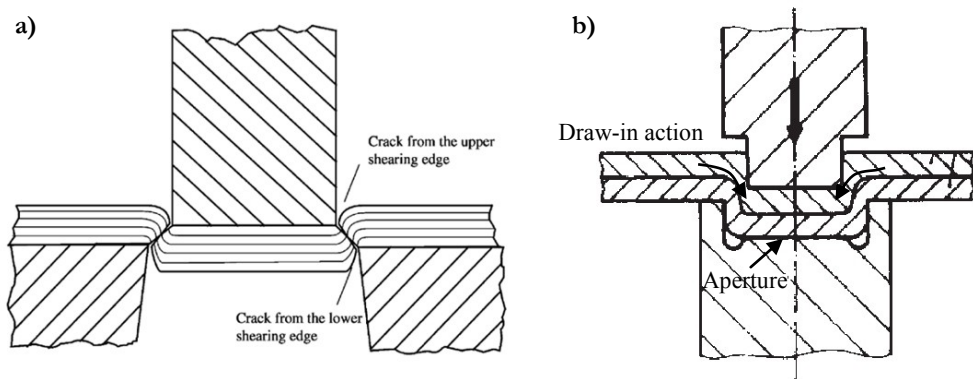

Fig. 34 a) Principle of sheet metal cutting by shearing process showing the mechanisms of crack propagation [50] b) Schematic showing draw-in action founded in typical mechanical clinching and sheet metal cutting [51].

In sheet metal cutting by shearing process, sheet bending action is caused by draw-in action (shown in Fig.34b) which draws the upper sheet into the aperture (softened thermoplastic in this case) and continues until the bending resistance is high enough for shear fracture to start [52]. The depth of sheet rollover and the height of burr increase with increasing cutting clearance [50]. During the tool is being driven into the work-piece, a mixture of material softening and work hardening occur simultaneously. The occurrences of these phenomena directly depend on temperature of material, strain rate and physical properties of material. It is also noted that welding parameters especially travel speed play a significant role on the amount of these factors which control the deformation during FSW.

4.7 Mechanical test

The strength of aluminum-thermoplastic hybrid joints were evalutated by lap shear testing on an Instron 4505 testing machine. Three effects of welding parameters on the joint strength including effect of travel speed, rotational direction and shoulder geometries were investigated. The results of tensile strength of joints made by AA5754 and polypropylene are graphically represented in Fig.35. The maximum tensile strength of hybrid joints is approximately 845 N from joint 5b using the scroll shoulder tool.

The mechanical test results in Fig. 35 indicated that the tensile strength of hybrid joints is strongly affected by a change in tool travel speed. It can be obviously seen from the scatter plot in Fig. 36 that the strength of joint welded with a low travel speed (3C) is significatly higher than the one welded using a high travel speed (3E) for concave shoulder tool under the same welding parameters. The relatively low tensile strength of specimen 3E may result from the formation of groove-like defect at the retreating side of the weldment as shown in Fig. 37b. A lack of material filling at the retreating side causes a reduction of polypropylene sheet cross section; as a result, the joint strength will be reduced when the tensile test is performed. The so-called necking of thermoplastic sheet leads to a weaker interface fracture between the weldment and aluminum alloy sheet. This is the result of higher bending action when the sheet cross section is small.
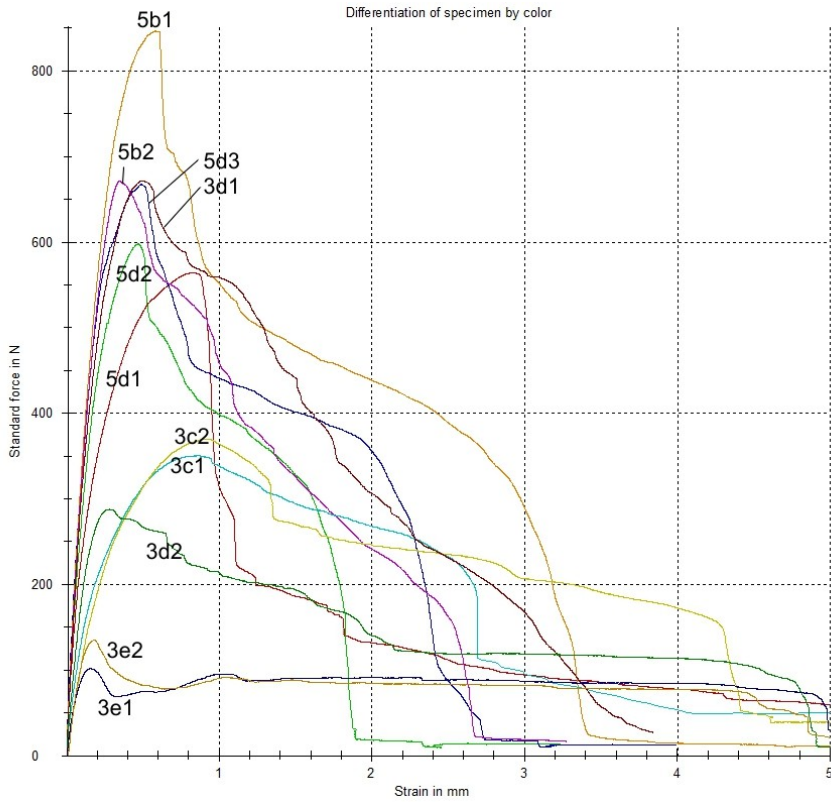
Fig. 35 The tensile strength of AA5754-Polypropylene joint welded by various welding condition. The joint "5d" gives the maximum tensile strength of 845 N which was made using the scroll shoulder tool.
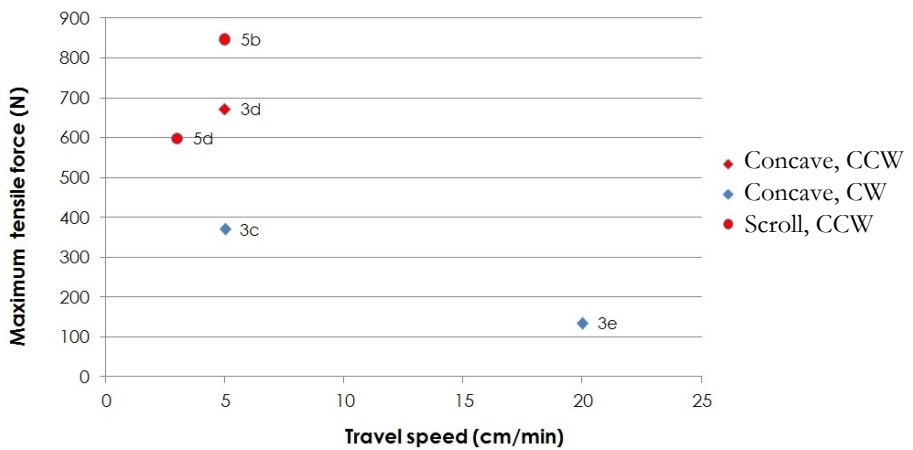

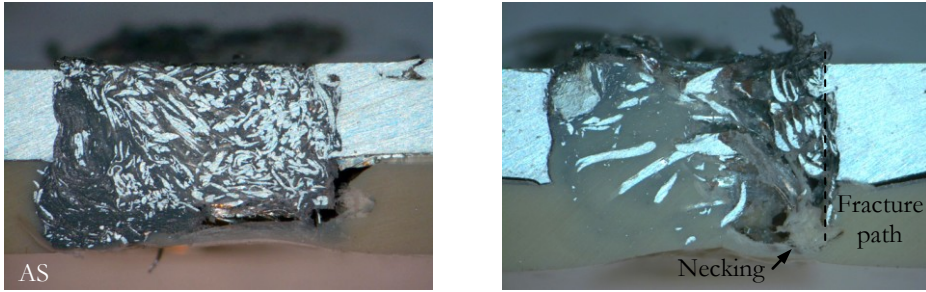Fig. 36 The scatter plot of maximum tensile force versus travel speed.

Fig. 37 The micrographs of AA5754-PP joint cross sections. a) specimen 3C (1800 rpm, 5 cm/min, 0.5°, CW b) specimen 3E (1800 rpm, 20 cm/min, 0.5°, CW).

The effects of rotational direction on the value of tensile strength can be investigated by considering the schematic in Fig. 38. The joint welded using CCW rotational direction has higher tensile strength compared with the joint welded using another direction for all tool geometries. The consistent microstructure investigation in Fig. 39 showed that a large worm-hole defect can be found in the specimen welded using CW rotational direction. While there is only small void defects can be detected from the joint welded using CCW rotational direction. Fig 39a-39b schematically show the different fracture paths of specimens welded using CW and CCW rotational direction. The fracture surfaces of welds after lap shear test presented two distinct failure modes including interfacial mode and pull-out mode occurred during the tensile test as can be seen in Fig 39c-39d. The unsatisfactory defect position and shape due to abnormal stirring when the tool rotates in CW direction significantly reduces the strength of hybrid joint. It is evident from the figure that the failure of weld is initiated near the tip of the worm-hole defect and continuously propagated along the nugget until the weld is torn off. This failure mechanism has relatively low energy failure which results in a low maximum tensile load under the lap shear test compared to other failure mechanisms.
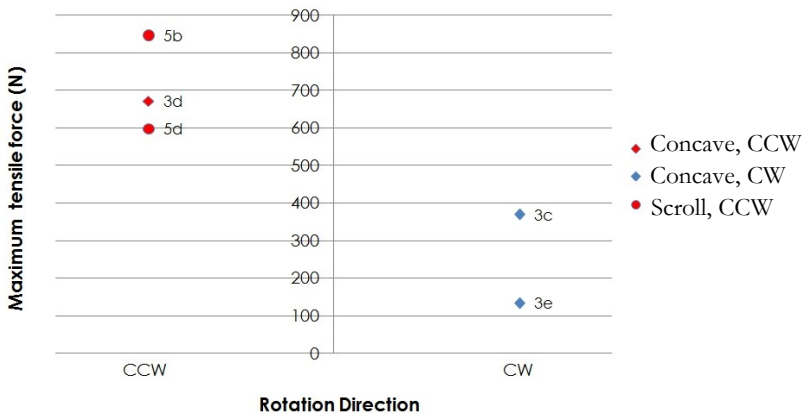

Fig. 38 The scatter plot of maximum tensile force of various tools in both rotation direction.
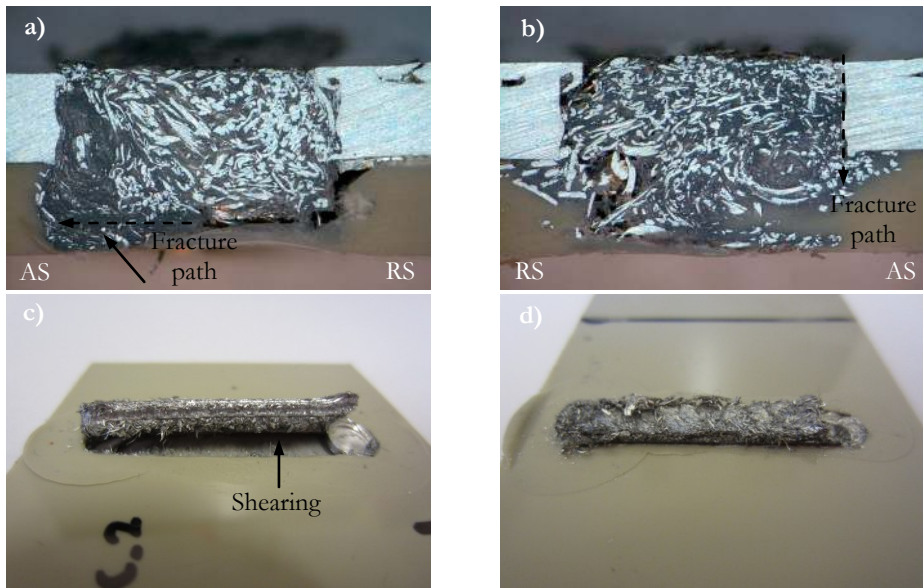
Fig. 39 a) AA5754-PP joint cross sections welded with 1800 rpm, 5 cm/min, 0.5°, CW b) AA5754-PP joint cross sections welded with 1800 rpm, 5 cm/min, 0.5°, CCW c) fracture surface of joint in Fig 39a. d) fracture surface of joint in Fig 39b.

The scatter plot in Fig. 41 presents the maximum tensile load as well as strain at the peak load of specimens welded by various welding conditions. It can be seen from the figure that sample "5b" which was weld using scroll shoulder tool has a highest toughness among all tested samples. The fracture surface of this specimen in Fig. 40a, b revealed that the zone near the metal-weldment interface contains an amount of thermoplastic matrix without aluminum fragments. This pure thermoplastic zone may result in an enhancement of interface bonding between aluminum sheet and weldment which subsequently increases the maximum tensile load of tested specimen. It is also noticed from the results that this pure thermoplastic matrix zone can be visibly found in the sample "5b" only. It can also be seen in Fig 40 that the region with melted thermoplastic material outside the stir zone is exceptionally large. This large bonding area can contribute to the high strength in this case.
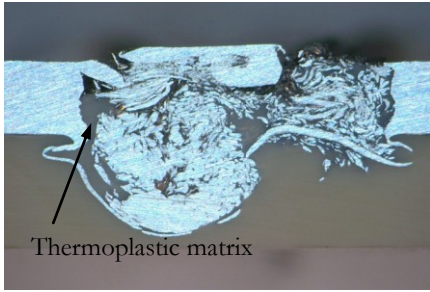
Fig.40 AA5754-PP joint cross section and fracture welded with 1500 rpm, 5 cm/min, 0.5°, CCW
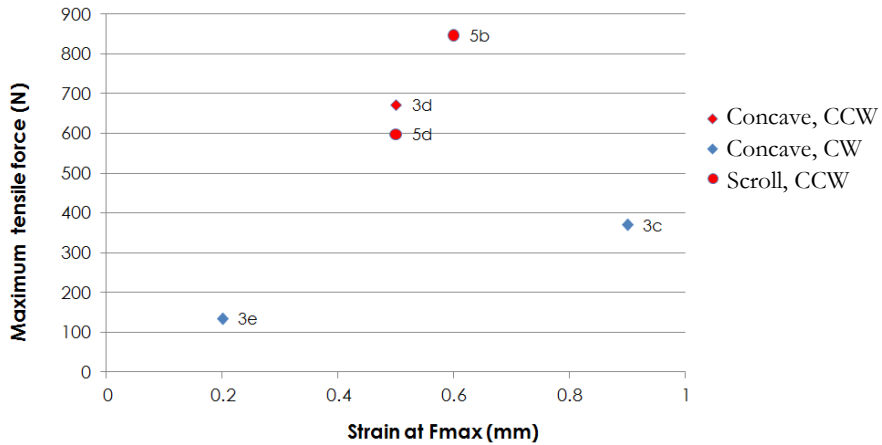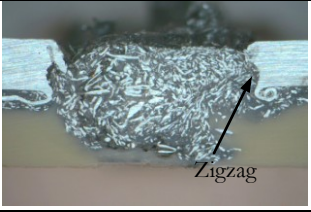

Fig. 41 The scatter plot of maximum tensile force versus strain at maximum tensile load.

4.8 Failure analysis

Table 5.2 summarized the fracture surface characteristics, fracture modes as well as mechanical test results of lap shear specimens which had been done in this thesis. High tensile force was obtained when the samples were failed by pull-out fracture mode which has highest failure energy. The metallographic examination in Table 5.2 showed that the presence of zigzag interface between aluminum alloy sheet and weldment enhances the maximum tensile force of sample which can be seen in case of sample 5b and 5d. A larger bonding area of weld nugget due to the zigzag interface results in an increase in weld strength of pull-out effect during specimen failure. This large bonding area of weld nugget coupling with a presence of thermoplastic matrix at external stir zone significantly increase the bonding strength of weld and produce the joint with the highest tensile strength (5b). Indeed, the tensile force is also increased by the mechanical locking effect between aluminum alloy sheet and weldment caused by the locking effect between zigzag feature and melted thermoplastic.

Table 5.2 Failure analysis tables

Sample	F_m (N)	Strain at max (mm)	Interface feature	Fracture mode	Cross section
3c	370.1	0.9	Plain	Shear	
3d	671.5	0.5	Plain	Pull-out	
3e	134.7	0.2	Plain	Pull-out	
5b	846.7	0.6	Zigzag	Pull-out	
5d	597.9	0.5	Zigzag	Pull-out	

Note: F_m is the maximum tensile force of tested sample

5. SUMMARY

5.1 Conclusion

Friction stir welding was used to join aluminum alloy sheets to thermoplastics. Two aluminum alloys were studied – one AA5000 and one AA6000 alloy. A range of thermoplastic materials were studied including, PP, PA12 and PET. Two materials with fibre reinforcement were also studied with PA-glass fibre and PET –PET fibre. Joints were created by friction stir welding with the tool contacting on the aluminum side. The effect of different process parameters was studied both by evaluation sections through the joints and with lap shear mechanical tests. The results of the studies can be concluded as follows;

- Joints were created by generating a stir zone of aluminum chips which was filled with melted thermoplastic entering from below.
- A number of defects could be identified in the joint zone like cavities, regions with very large or no chips. Flash of different extent on the top side of the aluminum alloys was also observed. The melted plastic could penetrate into the interface between aluminum alloy and thermoplastic to different degrees.
- The most important process parameters were pin geometry and thread, translation speed and rotation direction. They all had a significant effect on presence of defects in the joints. Relatively low travel speed and counter clockwise rotation was favoured.
- The most successful joints were created with scroll shoulder tool, right-hand thread pin rotating in counterclockwise rotational direction.
- Typical process parameters with good joint results were pin length 1.5 times the aluminum sheet thickness, cylindrical threaded pin, translation speed of 5 cm/min and counterclockwise rotation at a speed of 1800 rpm.
- Lap shear strengths were recorded up to 846N with a joint width of 40 mm. The elongations to failure were up to 0.9 mm.
- Voids or groove-like defect are caused by a lack of material circulation and insufficient amount of material to fill up the weld cavity due to the material loss from ejected aluminum chips/flash formation.
- Flash are caused by an excess contact pressure between the shoulder and work-piece top surface which is a result of a large tool tilt angle. Flash can be reduced by the action of shoulder geometries such as using scroll shoulder tool
- Aluminum chip morphology and chip size are controlled by so-called weld pitch which is the ratio of travel speed to rotation speed. Low weld pitch

welding produces the welds with small void formation and finer aluminum fragments compared to the welds using a high weld pitch.

- Tool rotational direction controls the direction of material flow inside the weld cavity. Using CW rotational direction is not preferable due to a loss of material through a work-piece surface.
- A moderate material mixing is more desirable due to its low void formation as well as good material circulation in the weld cavity.

REFERENCES

[1] M. Didi, P. Mitschang, Development of a Spot Welding Head for the Discontinuous Induction Welding of Metal/Fiber Reinforced-Plastic Joints, Institut für Verbundwerkstoffe GmbH, Kaiserslautern ,Germany.

[2] R. D. Adams, Adhesive Bonding, Woodhead Publishing (2005), Cambridge, UK.

[3] S. Amancio-Filho, J. dos Santos, Joining of Polymers and Polymer-Metal Hybrid Structures: Recent Developments and Trends, Polymer Engineering and Science 49 (2009):8, pp.1461-1476.

[4] S. Amancio-Filho, J. dos Santos, Mat.-wiss. u. Werkstofftech.(2008), pp. 799.

[5] T. Nelson, C. Sorensen, C. Johns, S. Strand, J. Christensen, Proceedings of the 2nd International Symposium on FSW (2000), Gothenburg, Sweden.

[6] R. Nandan, T. Debroy, H. Bhadeshia, Recent Advances in Friction Stir Welding – Process, Weldment Structures and Properties, Progress in Materials Scince 53 (2008), pp.980-1023.

[7] R. Mishra, M. Mahoney, Friction Stir Welding and Processing, ASM International (2007), OH, USA.

[8] W. Thomas, R. Dolby, Friction Stir Welding Developments, 6th International Trends in Welding Research, ASM International (2003), OH, USA.

[9] R. Mishra, Z. Ma, Friction stir welding and processing, Materials Science and Engineering R 50 (2005), pp. 1-78.

[10] W. Thomas, S. Lockyer, S. Kalee, D. Staines, Friction Stir Welding-An Update on Recent Developments, A Paper Presented at ImechE Stressed Components in Aluminum Alloy (2003), Birmingham, UK.

[11] G. Cantin, S. David, W. Thomas, E. Lara-Curzio, S. Babu, Friction Skew-stir Welding of Lap Joints in 5083-O Aluminum, Science and Technology of Welding and Joining 10 (2005):3, pp. 268-280.

[12] G. Zhang, W. Su, J. Zhang, Z. Wei, J. Zhang, Effects of Shoulder on Interfacial Bonding During Friction Stir Lap Welding of Aluminum Thin Sheets Using Tool Without Pin, Transaction of Nonferrous Metals Society of China 20 (2010), pp.2223-2228.

[13] H. Badarinarayan, F. Hunt, K. Okamoto, Friction Stir Welding and Processing, ASM International (2007), OH, USA.

[14] T. Iwashita, Method and Apparatus for Joining, U.S. Patent 6,601,751 (2003)

[15] C. Shilling, J. dos Santos, Method and Device for Joining at Least Two Adjoining Work Pieces by Friction Welding, U.S Patent Application 2002/0179682 (2002).

[16] K. Okamoto, F. Hunt, S. Hirano, Development of Friction Stir Welding Technique and Machine for Aluminum Sheet Metal Assembly, SAE Technical Paper 2005-01-1254 (2005).

[17] H. Badarinarayan, Q. Yang, S. Zhu, Effect of Tool Geometry on Static Strength of Friction Stir Spot-welded Aluminum Alloy, International Journal of Machine Tools & Manufacture 49 (2009), pp.142-148.

[18] S. Hirasawa, H. Badarinarayan, K. Okamoto, T. Tomimura, T. Kawanami, Analysis of Effect of Tool Geometry on Plastic Flow During Friction Stir Spot Welding Using Particle Method, Journal of Materials Processing Technology 210 (2010), pp.1455-1463.

[19] A. Addison, A. Robelou, Proceeding of 5th International Friction Stir Welding Symposium (2004), TWI, Metz, France.

[20] Z. Feng, M. Santella, S. David, R. Steel, S. Packer, T. Pan, M. Kuo, R. Bhatnagar, Friction Stir Spot Welding of Advanced High Strength Steels-A Feasibility Study, SAE Technical Paper 2005-01-1248 (2005).

[21] K. Aota, K. Ikeuchi, Development of Friction Stir Spot Welding Using Rotating Tool without Probe and Its Application to Low Carbon Steel Plates, Quarterly Journal of the Japan Welding Society 26 (2008), pp. 54-60.

[22] Y. Tozaki, Y. Uematsu, K. Tokaji, A Newly Developed Tool Without Probe for Friction Stir Spot Welding and Its Performance, Journal of Materials Processing Technology 210 (2010), pp. 844-851.

[23] D. Bakavos, Y. Chen, L. Babout, P. Prangnell, Material Interactions in a Novel Pinless Tool Approach to Friction Stir Spot Welding Thin Aluminum Sheet, Metallurgical and Materials Transaction A 42A (2011), pp.1266-1282.

[24] Y. Uematsu, K. Tokaji, Y. Tozaki, T. Kurita, S. Murata, Effect of Re-filling Probe Hole on Tensile Failure and Fatigue Behaviour of Friction Stir Spot Welded Joints in Al-Mg-Si Alloy, International Journal of Fatigue 30 (2008), pp.1956-1966.

[25] M. Troughton, Handbook of Plastics Joining - A Practical Guide, William Andrew Publishing (2008), NY, USA.

[26] T. Nelson, C. Sorenson, C. Johns, Friction Stir Welding of Polymeric Materials, U.S Patent 6,811,632 B2 (2004).

[27] C. Ageorges, Y. Lin, H. Meng, Advances in Fusion Bonding Techniques for Joining Thermoplastic Matrix Composites: A Review, Composites Part A: Applied Science and Manufacturing 32 (2001):6, pp.839-857.

[28] Z. Kiss, T. Czigany, Applicability of friction stir welding in polymeric materials, Periodica Polytechnica: Mechanical Engineering 51 (2007):1, pp.15-18.

[29] A. Scialpi, M. Troughton, S. Andrews, L. De Fillippis, Viblade™ : Friction Stir Welding for Plastics, Welding International 23 (2009):11, pp.846-855.

[30] Z. Tadmor, C. Gogos, Principles of Polymer Processing, John Wiley & Sons (1979), NY, USA.

[31] S. Amancio-Filho, C. Bueno, J. dos Santos, N. Huber, E. Hage Jr., On the Feasibility of Friction Spot Joining in Magnesium/Fiber-reinforced Polymer Composite Hybrid Structures, Material Science and Engineering A 528 (2011), pp. 3841-3848.

[32] S. Krüger, G. Wagner, D. Eifler, Ultrasonic Welding of Metal/Composite Joints, Advanced Engineering Materials 6 (2004):3, pp.157-159.

[33] F. Balle, G. Wagner, D. Eifler, Ultrasonic Metal Welding of Aluminum Sheets to Carbon Fibre Reinforced Thermoplastic Composites, Advanced Engineering Materials 11 (2009):1-2, pp. 35-29.

[34] T. Massalski, Binary Alloy Phase Diagrams 2nd Edition, ASM International (1990), OH, USA.

[35] F. Balle, S. Huxhold, G. Wagner, D. Eifler, Damage Monitoring of Ultrasonically Welded Aluminum/CFRP-Joints by Electrical Resistance Measurements, Procedia Engineering 10 (2011), pp.433-438.

[36] W.Y. Chien, J. Pan, and P. Friedman, Failure of Laser Welds in Aluminum Sheets, SAE Technical Paper 2001-01-0091 (2001).

[37] A.K. van der Vegt and L. Govaert, Polymeren, van keten tot kunstof, Delft University Press, Delft, The Netherlands.

[38] J. Mark, Physical Properties of Polymers Handbook, Springer Science and Business Media (2007), NY, USA.

[39] B. Åström, Manufacturing of Polymer Composites, Chapman and Hall (1997), London, UK.

[40] ASTM D1002-05, Standard Test Method for Apparent Shear Strength of Single-Lap-Joint Adhesively Bonded Metal Specimens by Tension Loading (Metal-to-Metal), ASTM International (2005), Berlin, Germany.

[41] H. Atharifar, D. Lin, R. Kovacevic, Numerical and Experimental Investigations on the Loads Carried by the Tool During Friction Stir Welding, Journal of Materials Engineering and Performance 18 (2009), pp. 339-350.

[42] L. Fratini, G. Buffa, D. Palmeri, J. Hua, R. Shivpuri, Material Flow in FSW of AA7075-T6 Butt Joints: Numerical Simulations and Experimental Verifications, Science and Technology of Welding and Joining 11 (2006), pp.412-421.

[43] M. Soron, Robot System for Flexible 3D Friction Stir Welding, Doctoral Dissertation, Orebro University (2007), Orebro, Sweden.

[44] Y. Kim, H. Fujii, T. Tsumura, T. Komazaki, K. Nakata, Three Defect Types in Friction Stir Welding of Aluminum Die Casting Alloys, Material Science and Engineering A 415 (2006), pp. 250-254.

[45] K. Kumar, S. Kailas, The Role of Friction Stir Welding Tool on Material Flow and Weld Formation, Materials Science and Engineering A 485 (2008), pp. 367-374.

[46] W. Arbegast, Hot Deformation of Aluminum Alloys III, TMS (2003), Warrendale, PA, USA.

[47] R. Nandan, G. Roy and T. DebRoy, Numerical Simulation of Three Dimensional Heat Transfer and Plastic Flow during Friction Stir Welding of Aluminum Alloys, Metallurgical and Materials Transactions A 37 (2006), pp. 1247-1259.

[48] H. Chen, K. Yan, T. Lin, S. Chen, C. Jiang, Y. Zhao, The Investigation of Typical Welding Defects for 5456 Aluminum Alloy Friction Stir Welds, Material Science and Engineering A 433 (2006), pp. 64-69.

[49] A. Nunes Jr., Metal Flow in Friction Stir Welding, Proceeding of the Material Science and Technology Conference (2006), OH, USA, pp. 1375-1386.

[50] T. Hilditch, P. Hodgson, Development of the Sheared Edge in the Trimming of Steel and Light Metal Sheet Part 1-Experimental Observations, Journal of Materials Processing Technology 169 (2005), pp.184–191.

[51] S. Gao, L. Budde, Mechanism of Mechanical Press Joining, International Journal of Machine Tools and Manufacture 34 (1994):5, pp.641-657.

[52] G. Bing, J. Wallbank, The Effect of Using a Sprung Stripper in Sheet Metal Cutting, Journal of Materials Processing Technology 200 (2008), pp.176-184.